Deep-Sea Research II ▮ (▮▮▮▮) ▮▮▮–▮▮▮

Contents lists available at ScienceDirect

Deep-Sea Research II

journal homepage: www.elsevier.com/locate/dsr2

# Impacts on phytoplankton dynamics by free-drifting icebergs in the NW Weddell Sea

M. Vernet [a,*], K. Sines [b], D. Chakos [c,1], A.O. Cefarelli [d,2], L. Ekern [e,3]

[a] Scripps Institution of Oceanography, 8615 Discovery Way, La Jolla, CA, 92037, USA
[b] University of Georgia, 141 Marine Sciences Bldg., Athens, GA 30605, USA
[c] Scripps Institute of Oceanography, 8615 Discovery Way, La Jolla, CA 92037, USA
[d] Departamento Científico Ficología, Facultad de Ciencias Naturales y Museo, Universidad Nacional de La Plata, Paseo del Bosque s/n, 1900 La Plata, Argentina
[e] Raytheon Polar Services, 7400 S Tucson Way, Centennial, CO 80112, USA

ARTICLE INFO

*Article history:*
Received 12 November 2010
Accepted 12 November 2010

*Keywords:*
Phytoplankton
Icebergs
Primary production
Biomass
Size-Fractionated Chlorophyll

ABSTRACT

Glacier ice released to the oceans through iceberg formation has a complex effect on the surrounding ocean waters. We hypothesized that phytoplankton communities would differ in abundance, composition and production around or close to an iceberg. This paper tests the influence of individual icebergs on scales of meters to kilometers, observed through shipboard oceanographic sampling on March-April 2009. Surface waters (integrated 0-100 m depth, within the euphotic zone) sampled close to the iceberg C-18a ($<1$ km) were characterized by lower temperatures, more dissolved nitrate, less total chlorophyll a (chla) concentration, less picoplankton ($<3$ μm) cell abundance, and higher transparency than surface conditions 18 km upstream. However, enrichment of large cells, identified as diatoms, was the basis of an active food chain. Upward velocity of meltwater and dissolved Fe concentrations in excess of 1-2 nM are expected to facilitate diatom specific growth. The presence of diatoms close to the iceberg C-18a and the higher variable fluorescence (Fv/Fm) indicated healthy cells, consistent with Antarctic waters rich in micronutrients. Furthermore, chla increased significantly 2 km around the iceberg and 10 days after the iceberg's passage. We hypothesize that the lower biomass next to the iceberg was due to high loss rates. Underwater melting is expected to dilute phytoplankton near the iceberg by entraining deep water or by introducing meltwater. In addition, high zooplankton biomass within 2 km of the iceberg, mainly Antarctic krill *Euphausia superba* and salps *Salpa thompsonii*, are expected to exert heavy grazing pressure on phytoplankton, the krill on large cells $>10$ μm and the salps on smaller cells, 3-10 μm. The iceberg's main influence in the austral fall is measured not so much by phytoplankton accumulation but by reactivation of the classic Antarctic food chain, facilitating diatom growth and sustaining high Antarctic krill populations.



## 1. Introduction

Sea ice, doubling the size of Antarctica every winter, is known to favorably affect water-column microbial communities in spring and summer through the marginal ice zone (Smith and Nelson, 1985). Similarly, glacier ice released to the oceans through iceberg formation could influence the water column and positively affect the biology through several physical-chemical processes. Although large icebergs such as the B-15 (295 km long × 40 km wide) off the Ross Ice Shelf affect the local pack ice dynamics by decreasing incident light and consequently decreasing seasonal primary production by as much as 40% (Arrigo et al., 2002), smaller icebergs (of the order of several km or less) that move along the Antarctic coastal current (Gladstone et al., 2001) seem to have a positive effect on phytoplankton (Smith et al., 2007).

Primary production in Antarctic coastal areas may be limited by light (Mitchell and Holm-Hansen, 1991), zooplankton grazing (Walsh et al., 2001) or micronutrients such as Iron (Fe) (Martin et al., 1990; Boyd et al., 2000). Phytoplankton community composition responds to changes in water-column stability as well as Fe or Ammonium ($NH_4^+$) enrichment (Martin et al., 1990). As observed during seasonal succession, microplankton cells ($>20$ μm) can dominate in productive waters during the spring bloom and along the ice edge while flagellates and microflagellates, many of them nanoplanktonic (2-20 μm), are abundant in less productive environments or later in the season (reviewed by Knox, 2007). Diatoms and/or the colonial prymnesiophyte

* Corresponding author. Tel.: +1 858 534 5322 fax: +1 858 534 2997.
*E-mail addresses:* mvernet@ucsd.edu (M. Vernet), kariesines@att.net (K. Sines), acefarelli@fcnym.unlp.edu.ar (A.O. Cefarelli), lindsey.ekern@gmail.com (L. Ekern).
[1] Tel: +1 858 534 8086 ; fax: +1 858 534 2997.
[2] Tel.: +54 2 2 1 425 7744x128.
[3] Tel.: +1 408 480 4285.

0967-0645/$ - see front matter © 2011 Elsevier Ltd. All rights reserved.
doi:10.1016/j.dsr2.2010.11.022

*Phaeocystis* spp. are major contributors to autotrophic organic carbon during periods of high productivity (Fryxell and Kendrick, 1988), and potentially, around icebergs (Whitaker, 1977). As the dynamics of upwelling and water-column stabilization in the vicinity of icebergs are expected to be similar to those observed in the marginal ice zone (Dunbar, 1984) we can also expect to detect changes in community composition around the iceberg, as compared to background water. The similarity with the ice edge is, however, limited, as no ice algal seeding is expected from icebergs (but see Roberts et al., 2007). Phytoplankton composition can be affected by grazing pressure as well; diatom biomass from the Weddell Sea can be grazed down and replaced by a community composed of flagellates such as cryptomonads and *Pyramimonas* (Hegseth and Von Quillfeldt, 2002; Froneman et al., 2004). Shelf waters of the Western Antarctic Peninsula present similar dynamics (Garibotti et al., 2003a; Walsh et al., 2001).

Although only a limited number of studies exist concerning the impact of icebergs on the microbial community in the Antarctic, the few available studies from the Arctic and Antarctic have yielded contradictory results. While Shulenberger (1983) did not find any increase in phytoplankton biomass around Arctic icebergs, others have found increased phytoplankton and seabirds associated with them (Hooper, 1971). Two factors that have been consistently studied are degree of drifting and iceberg size. Grounded icebergs seem to create a more productive system in their area of influence, while no such effect has been detected in drifting icebergs. Extremely large icebergs seem to decrease regional production due to decreased free surface between ocean and atmosphere (i.e., Arrigo et al., 2002) while a positive effect is expected for smaller icebergs due to the nutrient enrichment and contribution of freshwater. Recently, a study by Smith et al. (2007) showed increased biological activity of phytoplankton, zooplankton and birds attributed to the presence of free-floating icebergs. High micronutrient concentrations originating from sediments associated with the icebergs, capable of sustaining healthy phytoplankton, suggested icebergs are an important source of micronutrients to Antarctic coastal waters (Lancelot et al., 2009) as has previously been shown for oceanic waters (de Baar, 1995).

We hypothesized that phytoplankton around or close to the iceberg would show different properties than plankton away from the iceberg's influence. Phytoplankton communities would differ in abundance, composition and production. Changes in phytoplankton could occur at two different spatial scales: (i) around an individual iceberg where a gradient of primary production could develop perpendicular to the iceberg or on the iceberg plume, and (ii) on a regional scale, in the area affected by iceberg drift, such as the "iceberg alley" in the Weddell Sea. This paper presents a test of the influence of individual icebergs on scales of meters to kilometers, studied with oceanographic sampling on board ships. Non-impacted waters serve as control sites.

## 2. Materials and Methods

Waters surrounding the iceberg and control areas away from the iceberg's influence were sampled for phytoplankton distribution, primary production and nutrients. Sampling for the Iceberg III cruise was conducted on board the ARSV Nathaniel B. Palmer in the Powell Basin, NW Weddell Sea, from 10 March through 7 April 2009 while iceberg C-18a was free-drifting between 61° and 62°S and between 49° and 52°W (Fig. 1, Table 1). The overall water depth during the sampling ranged from 1600 to 3277 m. C-18 originated in the Ross Ice Shelf in 2002. C-18a, which is derived from it, was tracked between Julian Day 152, 2005 and Julian Day 326, 2009 (Stuart and Long, this issue). The iceberg was sampled at a distance of $<1$ km for waters impacted (Close C-18a) and at $>74$ km to the East as a control (Control Station, CS). We also sampled at 16-18 km on the iceberg's projected path as a proximate control (Far C-18a). A fourth location, the Iceberg Alley (IA), was sampled $>130$ km to the South East of C-18a; it represented an area of high iceberg density.

Water samples were taken with a Conductivity-Temperature-Depth (CTD) rosette on the ship, outfitted with 24 8.5-L Niskin bottles, a Wetlabs ECO fluorometer and a C-Star transmissometer from Wetlabs. To estimate biomass, samples were taken at 10-12 depths from 0-500 m. For primary productivity we sampled within the euphotic layer, at depths corresponding to 100%, 50%, 25%, 10%, 5% and 1% of incident irradiance. The euphotic zone ($Z_{eu}$) was defined as the layer of water above the 1% surface irradiance. To determine the sampling depths, we used a Biospherical Instruments QSP-200 L attached to the CTD rosette, away from shading effects. Mixed-layer depth (MLD) was calculated as the depth where the change in water-column density $>0.01$ within a 5-m layer.

Nutrient concentrations were determined by flow injection analysis using a Lachat Instruments Quikchem 8000 Autoanalyzer. Samples were collected directly from the Niskin bottles; samples not processed at time of collection were frozen and stored at $-20$ °C until analysis (usually for a few days). If frozen,

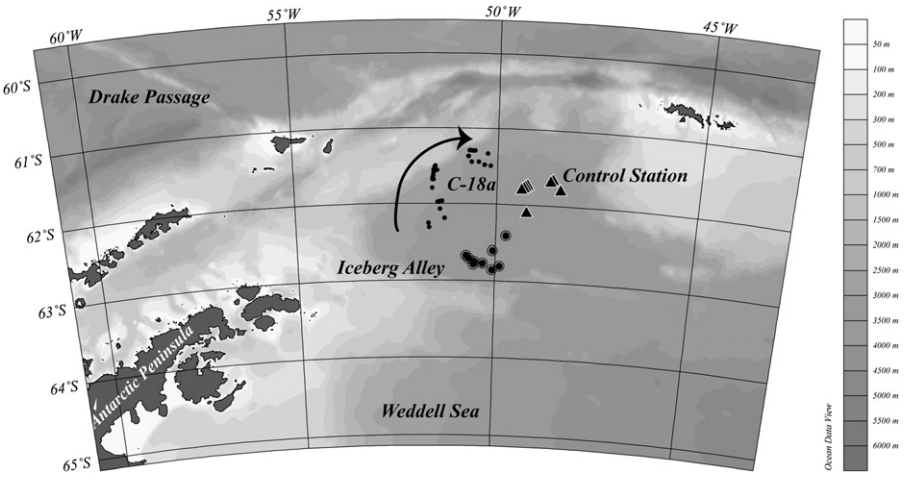


**Fig. 1.** : Map of Powell Basin in NW Weddell Sea, showing the locations of the stations sampled between 10 March and 7 April 2009: the C-18a iceberg (single black dots), the Iceberg Alley area (filled black circles), and the Control Station site (triangles). Arrow depicts C-18a drift from 10-30 March.

Please cite this article as: Vernet, M., et al., Impacts on phytoplankton dynamics by free-drifting icebergs in the NW Weddell Sea. Deep-Sea Research II (2011), doi:10.1016/j.dsr2.2010.11.022

**Table 1**
Geographical and physical properties of stations sampled during the Iceberg III cruise. Abbreviations include Temp (temperature), Fluor (fluorescence), and Trans (transmission measured as beam attenuation). Data is averaged over the top 100 m sampled and is presented ± one standard deviation. For each sampling region, the overall average and standard deviations are also presented beneath each sampling region. Locations that are significantly different from Close C-18a are marked in bold ($\alpha=0.05$) and in bold italics ($\alpha=0.1$).

| Event | Sampling Region | Date | Distance from iceberg (km) | Lat (°S) | Lon (°W) | Mixed Layer Depth (m) | Average Salinity | Average Temp (°C) | Average Density (kg m$^{-3}$) | Average Oxygen (ml l$^{-1}$) | Average Fluor (mg m$^{-3}$) | Average Trans (%) |
|---|---|---|---|---|---|---|---|---|---|---|---|---|
| 3 | Close C-18a | 3/10/2009 | 0.58 | 62.256 | 51.689 | 56 | 34.028 ± 0.260 | −0.610 ± 0.693 | 27.347 ± 0.239 | 7.37 ± 0.33 | 0.30 ± 0.15 | 96.55 ± 1.30 |
| 29 | Close C-18a | 3/16/2009 | 0.49 | 61.967 | 51.352 | 51 | 33.995 ± 0.264 | −0.441 ± 0.527 | 27.314 ± 0.235 | 7.32 ± 0.57 | 0.60 ± 0.27 | 96.04 ± 1.41 |
| 39 | Close C-18a | 3/17/2009 | 0.71 | 62.793 | 51.599 | 25 | 34.10 ± 0.170 | −0.775 ± 0.653 | 27.413 ± 0.164 | 7.24 ± 0.27 | 0.73 ± 0.21 | 96.47 ± 1.18 |
| 101 | Close C-18a | 3/29/2009 | 0.32 | 62.369 | 50.713 | 32 | 34.239 ± 0.086 | −0.725 ± 0.347 | 27.525 ± 0.084 | 7.02 ± 0.29 | 0.40 ± 0.16 | 96.81 ± 0.92 |
| 108 | Close C-18a | 3/30/2009 | 0.72 | 61.481 | 50.318 | 50 | 34.119 ± 0.121 | −0.347 ± 0.576 | 27.410 ± 0.123 | 7.28 ± 0.27 | 0.55 ± 0.24 | 95.67 ± 1.64 |
| | Average ± Standard Deviation | | | | | | 34.096 ± 0.095 | −0.58 ± 0.18 | 27.402 ± 0.081 | 7.25 ± 0.13 | 0.52 ± 0.17 | 96.31 ± 0.45 |
| 8 | Far C-18a | 3/11/2009 | 16.60 | 62.311 | 51.601 | 24 | 33.920 ± 0.307 | −0.460 ± 0.641 | 27.254 ± 0.275 | 7.40 ± 0.43 | 0.57 ± 0.22 | 96.17 ± 1.10 |
| 46 | Far C-18a | 3/18/2009 | 17.82 | 61.562 | 51.484 | 20 | 33.988 ± 0.201 | 0.083 ± 0.707 | 27.282 ± 0.194 | 7.44 ± 0.25 | 0.80 ± 0.35 | 95.15 ± 1.73 |
| 56 | Far C-18a | 3/20/2009 | 18.54 | 61.500 | 51.520 | 40 | 34.111 ± 0.176 | −0.199 ± 0.594 | 27.397 ± 0.170 | 7.24 ± 0.35 | 0.60 ± 0.26 | 95.57 ± 1.59 |
| 65 | Far C-18a | 3/20/2009 | 18.00 | 61.512 | 51.618 | - | 34.150 ± 0.080 | −0.185 ± 0.510 | 27.428 ± 0.089 | 7.29 ± 0.19 | 0.67 ± 0.26 | 95.38 ± 1.60 |
| 121 | Far C-18a | 4/1/2009 | 17.82 | 61.446 | 50.638 | 40 | 34.133 ± 0.155 | −0.289 ± 0.520 | 27.419 ± 0.148 | 7.41 ± 0.29 | 0.73 ± 0.28 | 95.27 ± 1.54 |
| | Average ± Standard Deviation | | | | | | 34.060 ± 0.101 | ***−0.210 ± 0.197*** | 27.356 ± 0.082 | 7.36 ± 0.09 | 0.68 ± 0.09 | ***95.51 ± 0.40*** |
| 147 | Iceberg Alley | 4/4/2009 | - | 62.806 | 49.883 | 45 | 34.145 ± 0.273 | −1.097 ± 0.340 | 27.464 ± 0.233 | 7.06 ± 0.60 | 0.43 ± 0.16 | 97.01 ± 0.93 |
| 154 | Iceberg Alley | 4/5/2009 | - | 62.858 | 50.073 | 32 | 34.197 ± 0.248 | −1.185 ± 0.249 | 27.509 ± 0.209 | 6.94 ± 0.63 | 0.45 ± 0.19 | 97.15 ± 0.97 |
| | Average ± Standard Deviation | | | | | | 34.171 ± 0.037 | **−1.141 ± 0.062** | 27.487 ± 0.032 | **7.00 ± 0.09** | 0.43 ± 0.02 | **97.08 ± 0.10** |
| 141 | Control Station | 4/3/2009 | - | 61.687 | 48.636 | 55 | 33.913 ± 0.200 | 0.023 ± 0.583 | 27.226 ± 0.187 | 7.47 ± 0.33 | 1.19 ± 0.39 | 94.80 ± 1.32 |
| 170 | Control Station | 4/7/2009 | - | 61.794 | 48.440 | 47 | 33.901 ± 0.177 | −0.089 ± 0.514 | 27.222 ± 0.165 | 7.52 ± 0.27 | 0.95 ± 0.35 | 95.00 ± 1.22 |
| | Average ± Standard Deviation | | | | | | **33.907 ± 0.009** | **−0.033 ± 0.079** | **27.224 ± 0.003** | 7.49 ± 0.03 | **1.07 ± 0.17** | **94.90 ± 0.14** |

samples were carefully defrosted in warm running water for ~1 h. The phosphate method was a modification of the molybdenum blue procedure of Bernhardt and Wilhelms (1967), in which phosphate was determined as a reduced phosphomolybdic acid employing hydrazine as the reductant. The nitrate+nitrite analysis used the basic method of Armstrong et al. (1967), with modifications to improve the precision and ease of operation. Sulfanilamide and N-(1-Napthyl) ethylenediamine dihydrochloride reacted with nitrite to form a colored diazo compound. For the nitrate+nitrite analysis, nitrate ($NO_3$) was first reduced to nitrite ($NO_2$) using a cadmium reduction column and imidazole buffer as described by Patton (1983). Nitrite analysis was performed on a separate channel, omitting the cadmium reductor. The silicic acid method was based on that of Armstrong et al. (1967) as adapted by Atlas et al. (1971). Addition of an acidic molybdate reagent formed silicomolybdic acid which was then reduced by stannous chloride. Ammonium was determined by an indophenol blue method modified from ALPKEM RFA methodology which references Methods for Chemical Analysis of Water and Wastes, March 1984, EPA-600/4-79-020, "Nitrogen Ammonia", Method 350.1 (Colorimetric, Automated Phenate).

Chlorophyll a (chla) concentration was estimated fluorometrically from extracted samples (Holm-Hansen et al., 1965). Water aliquots (120 or 250 ml) were filtered onto a membrane filter, frozen at −80 °C for at least 24 h and extracted in 90% acetone at −20 °C. Fluorescence was measured with a digital Turner Designs Model AU10. Calibration was done with pure chla (Sigma Co.) in 90% acetone (ACS grade) with concentration measured spectrophotometrically (Jeffrey and Humphrey, 1975). Chla was measured in 6 size fractions with 0.2, 1.0, 3.0, 5.0, 10.0 and 20.0-μm membrane polycarbonate filters (Osmonics). The chla retained by the 0.2-μm filter was considered total chla concentration. Chla in the different size fractions (in units of mg m$^{-3}$) is calculated by subtraction from the biomass retained by consecutive filters. Chla in the 0-100 m layer is integrated to represent average phytoplankton response within the euphotic zone due to iceberg processes (in units of mg m$^{-2}$). Integrated values are calculated from surface to 100 m depth with the trapezoid method.

Chla concentration was also measured with a Wetlabs ECO (Environmental Characterization Optics) fluorometer attached to a MOCNESS (Multiple Opening/Closing Net and Environmental Sensing System from BESS Inc.) net based on determinations of *in vivo* fluorescence by chla. Five locations, 0.4, 1.9, 9.3 and 18.5 km away from the iceberg were sampled from surface to 300 m (see Kaufmann et al. (this issue) for more details). All deployments were carried out at night (midnight to 5 am local time) so data from the different deployments are free of fluorescence quenching and comparable among each other. The *in vivo* fluorescence was calibrated by the manufacturer to equivalent mg chla m$^{-3}$. The data were averaged by 10 m depth and expressed as surface chla concentrations (0-10 m) in mg m$^{-3}$ and integrated chla (0-300 m) in units of mg m$^{-2}$, as explained above.

Cell abundance in three size fractions was measured by flow cytometry (cells < 3 μm, cells 3-10 μm and cells > 10 μm). Samples (1 ml) were preserved with 2% paraformaldehyde solution and kept at −80 °C until analysis. Analysis was performed at Bigelow Laboratory for Ocean Sciences at the J.J. MacIsaac Facility for Aquatic Cytometry. Concentrations are expressed as number of cells m$^{-3}$.

The degree of phytoplankton health (i.e. absence of stress) was estimated by its variable fluorescence (Fv/Fm), as measured by a FIRe System (Satlantic). Blanks were estimated from filtered seawater and reference fluorescence was estimated from extracted chla in 90% acetone. Samples were collected from the Niskin bottles upon CTD arrival on deck and stored in the dark at 4 °C for 15 min before analysis.

Estimates of primary production (SIS or Simulated In Situ experiments) were made experimentally at each CTD station, during 24-h on-deck incubations in UV opaque plexiglas (UV-O) incubators placed on a shade-free area on deck with temperature maintained at surface *in situ* conditions with running sea water (range from −1.5 °C to +1 °C). Duplicate 100-ml samples were incubated in 125-ml borosilicate bottles after addition of 5 μCi of $NaH^{14}CO_3$ per bottle. After 24 h, the samples were concentrated onto 25-mm Whatman GF/F filters, fumed with 20% HCl for 24 h and placed in

Please cite this article as: Vernet, M., et al., Impacts on phytoplankton dynamics by free-drifting icebergs in the NW Weddell Sea. Deep-Sea Research II (2011), doi:10.1016/j.dsr2.2010.11.022

5 ml of Universal scintillation fluid. Samples were then counted with a scintillation counter (Perkin Elmer Tri-Carb 2900 TRs). Specific activity of each sample depth was determined after $^{14}C$ inoculation from 0.1 ml of sea water fixed with 1 M NaOH. Time-zero values, determined from filtration of 100-ml sample before incubation, were always $<5\%$ of the light data. Primary production was calculated from the difference of light minus dark bottle readings and assuming a $HCO^{3-}$ in the water of 24,000 mg C $kg^{-1}$ (Carrillo and Karl, 1999). The efficiency of carbon uptake ($P^B$) was calculated as the integral of primary production divided by the integral of chla for the euphotic zone (Falkowski, 1980).

Due to the small sample size and shape of the distributions, non-parametric statistics were used to test differences between medians (Statistica version 5). Effects of the iceberg on surrounding waters was measured by comparing locations with respect to Close C-18a waters using the Mann-Whitney test; significance is presented at $\alpha=0.05$ and $\alpha=0.10$. Spearman rank order correlations were employed to establish relationships between paired measured variables within a location; significance was set at $\alpha=0.05$.

## 3. Results

Average temperature (0-100 m) was $-1.14\,^{\circ}C \pm 0.062$, $-0.58\,^{\circ}C \pm 0.183$, $-0.210\,^{\circ}C + 0.197$ and $-0.033\,^{\circ}C \pm 0.079$ (Table 1) defining a gradient of increasing temperatures from Iceberg Alley to the Control Station ($p<0.05$). Average transmission showed a comparable gradient of decreasing transparency (more suspended particles) while average salinity, density, oxygen and fluorescence did not show significant changes (Table 1).

Total phytoplankton biomass, estimated from chla abundance, was higher at Far C-18a (0.42 mg $m^3$) and the Control Station (0.45 mg $m^3$), intermediate at Close C-18a and lowest at Iceberg Alley (0.17 mg $m^3$) (Fig. 2, Table 2A). The chla in the different size fractions was higher in the mixed layer (0-50 m), decreasing exponentially below. In general, the chla at Far C-18a and the Control Station remained higher to 100 m while the Close C-18a and Iceberg Alley stations started to decrease at a shallower depth ($\sim$70 m). The picoplankton ($<3$ μm) fraction presented the highest concentration at the C-18a and Iceberg Alley sites (Fig. 2A, B, C) and was significantly lower at Close C-18a compared to Far C-18a (Table 2A). Highest concentration at the Control Station was associated with chla at 5-10 μm fraction (Fig. 2D). The larger size fraction of 10-20 μm chla presented a minimum at the surface and a maximum at $\sim$70-100 m depth at Close C-18a and Iceberg Alley and was more constant with depth in the other two locations (Fig. 2). The smaller fractions dominated the assemblage in the surface 100 m, with the exception of the Control Station where the intermediate fractions (3-5 μm and 5-10 μm) were more abundant (Table 2A). Total abundance was higher at Far C-18a (Fig. 2A and Table 2A). Phaeopigment concentration was on average $\sim$20% chla with some size fractions as high as 50% (Table 2B).

Waters sampled close to the iceberg (Close C-18a), integrated between 0-100 m depth, representative of the euphotic zone and subject to iceberg melting, were colder, with deeper mixed layers, more dissolved $NO_3$, less total chla concentration, less pico- ($<3$ μm) and nano- (5-10 μm) cell abundance and higher transparency than those 18 km upstream (Far C-18a) ($p<0.10$, Tables 1–4; Figs. 2 to 4). Large cells ($>10$ μm) were concentrated at 70-100 m, below the mixed layer; that peak was more conspicuous at Close C-18a (Fig. 4A). A similar pattern was observed at Iceberg Alley. Microphytoplankton (cells $>20$ μm) were higher at Close C-18a than at Far C-18a ($p<0.1$). In summary, the phytoplankton community influenced by the iceberg showed an enrichment of large cells and a concomitant decrease of small cells in surface waters, with a net effect of decreased total biomass $<1$ km from the iceberg. This is similar to the reported higher $>20$ μm chla/total chla for icebergs analyzed previously (Smith et al., 2007). Data from 2009 also showed large variability in the vicinity of the iceberg (Table 2).

The difference between the waters at Close C-18a and those at the Control Station was more striking. In addition to colder waters, with lower chla 1-10 μm, lower fluorescence and more transparency, the differences included lower cell abundance, higher salinity and more healthy cells (higher Fv/Fm) near the iceberg (Tables 1 to 4 and Figs. 2 to 4). Furthermore, more microphytoplankton were present in the 0-40 m mixed layer at C-18a compared to Far C-18a ($p<0.1$, Cefarelli et al.,

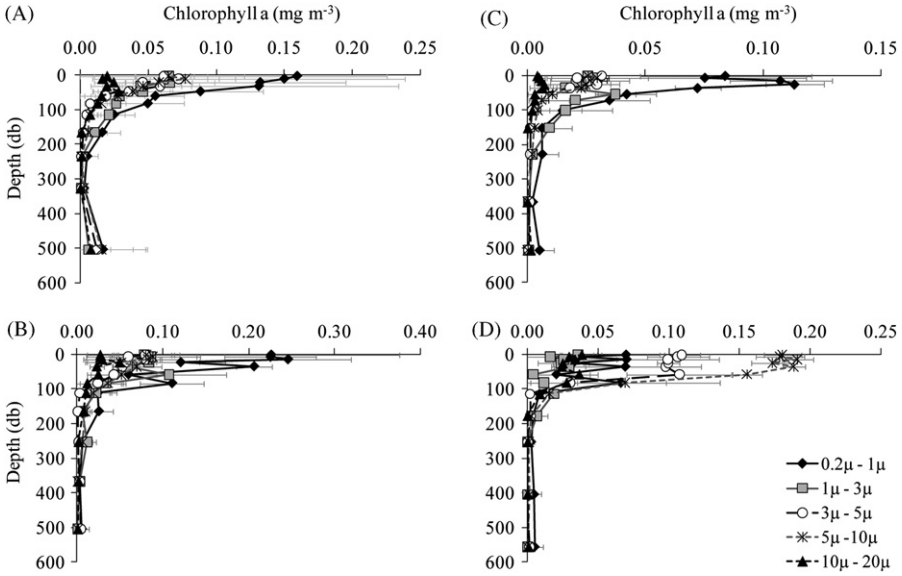


**Fig. 2.** Chlorophyll *a* profiles for each size fraction at the Close C-18a stations, $<1$ km from the iceberg (A), Far C-18a stations, 16–18 km NE of the iceberg (B), the Iceberg Alley stations (C) and the Control stations, 74 km East of C-18a (D). Data represents the average of all stations at a given location ($n=5$ for Close and Far C-18a, $n=2$ for Iceberg Alley and Control Station), and error bars represent one standard deviation from the mean. Data is plotted at the average depth for the location. Note different pigment scales for the different areas.

Please cite this article as: Vernet, M., et al., Impacts on phytoplankton dynamics by free-drifting icebergs in the NW Weddell Sea. Deep-Sea Research II (2011), doi:10.1016/j.dsr2.2010.11.022

**Table 2**
Chlorophyll a (Chla) and phaeopigment (Phaeo) size fraction within the euphotic zone. Data at each station represent the integrated to 100 m values and the mean and one standard deviation for each location is summarized beneath each sampling region. Locations that are significantly different from Close C-18a ( < 1 km from the iceberg) are marked in bold ($\alpha$=0.05) and in bold italics ($\alpha$=0.1). Number of samples in top 100 m was 6-8 depths.

| Event | Sampling Region | Total Chla (mg m$^{-2}$) | Chla 0.2 μ-1 μ (mg m$^{-2}$) | Chla 1 μ-3 μ (mg m$^{-2}$) | Chla 3 μ-5 μ (mg m$^{-2}$) | Chla 5 μ-10 μ (mg m$^{-2}$) | Chla 10 μ-20 μ (mg m$^{-2}$) | Chla > 20 μ (mg m$^{-2}$) |
|---|---|---|---|---|---|---|---|---|
| (A) | | | | | | | | |
| 3 | Close C-18a | 22.012 | 4.202 | 2.493 | 3.786 | 3.917 | 1.396 | 6.669 |
| 29 | Close C-18a | 27.154 | 7.576 | 3.804 | 4.032 | 6.144 | 1.557 | 4.105 |
| 39 | Close C-18a | 27.664 | 6.775 | 3.761 | 2.780 | 3.539 | 2.562 | 8.888 |
| 101 | Close C-18a | 19.877 | 8.090 | 4.572 | 1.759 | 1.677 | 1.238 | 3.314 |
| 108 | Close C-18a | 30.585 | 12.748 | 5.790 | 4.590 | 2.495 | 2.056 | 2.917 |
| Average ± Standard Deviation | | 25.458 ± 4.389 | 7.838 ± 3.106 | 4.084 ± 1.211 | 3.389 ± 1.122 | 3.554 ± 1.694 | 1.762 ± 0.543 | 5.179 ± 2.536 |
| 8 | Far C-18a | 27.113 | – | – | – | – | – | – |
| 46 | Far C-18a | 33.747 | 10.025 | 4.659 | 5.545 | 7.983 | 1.369 | 4.567 |
| 56 | Far C-18a | 29.836 | 10.570 | 5.208 | 3.716 | 3.749 | 2.834 | 3.790 |
| 65 | Far C-18a | 41.763 | 19.428 | 7.258 | 4.148 | 4.228 | 3.133 | 3.538 |
| 121 | Far C-18a | 34.034 | 9.591 | 8.494 | 3.642 | 5.559 | 1.625 | 5.501 |
| Average ± Standard Deviation | | **33.298 ± 5.537** | ***12.403 ± 4.700*** | **6.405 ± 1.787** | 4.263 ± 0.883 | 5.380 ± 1.897 | 2.240 ± 0.873 | 4.349 ± 0.884 |
| 147 | Iceberg Alley | 11.827 | 6.031 | 1.943 | 1.483 | 1.398 | 0.274 | 0.699 |
| 154 | Iceberg Alley | 12.849 | 5.862 | 2.855 | 1.155 | 1.709 | 0.613 | 0.685 |
| Average ± Standard Deviation | | **12.338 ± 0.723** | 5.947 ± 0.119 | ***2.339 ± 0.645*** | **1.319 ± 0.232** | ***1.554 ± 0.220*** | **0.443 ± 0.240** | 0.692 ± 0.010 |
| 141 | Control Station | 33.734 | 5.271 | 1.680 | 8.215 | 13.336 | 2.843 | 2.513 |
| 170 | Control Station | 27.532 | 3.270 | 1.403 | 6.175 | 12.630 | 2.240 | 1.796 |
| Average ± Standard Deviation | | **30.633 ± 4.385** | 4.270 ± 1.415 | **1.542 ± 0.196** | **7.195 ± 1.443** | **12.983 ± 0.499** | 2.542 ± 0.427 | 2.155 ± 0.507 |

| (B) Event | Sampling Region | Total Phaeo (mg m$^{-2}$) | Phaeo 0.2 μ–1 μ (mg m$^{-2}$) | Phaeo 1 μ-3 μ (mg m$^{-2}$) | Phaeo 3 μ-5 μ (mg m$^{-2}$) | Phaeo 5 μ-10 μ (mg m$^{-2}$) | Phaeo 10μ-20 μ (mg m$^{-2}$) | Phaeo > 20 μ mg m$^{-2}$) |
|---|---|---|---|---|---|---|---|---|
| 3 | Close C-18a | 6.037 | 1.866 | 1.238 | 0.702 | 0.891 | 0.281 | 1.089 |
| 29 | Close C-18a | 3.540 | 0.551 | 0.720 | 0.722 | 1.305 | 0.201 | 0.071 |
| 39 | Close C-18a | 8.332 | 2.751 | 1.545 | 0.578 | 1.535 | 0.664 | 1.444 |
| 101 | Close C-18a | 6.567 | 0.810 | 1.856 | 0.725 | 2.542 | 0.666 | 0.887 |
| 108 | Close C-18a | 7.222 | 1.486 | 1.868 | 0.605 | 1.871 | 0.601 | 0.901 |
| Average ± Standard Deviation | | 6.339 ± 1.784 | 1.493 ± 0.877 | 1.445 ± 0.481 | 0.667 ± 0.070 | 1.629 ± 0.622 | 0.482 ± 0.244 | 0.878 ± 0.504 |
| 8 | Far C-18a | - | - | - | - | - | - | - |
| 46 | Far C-18a | 7.867 | 1.696 | 1.009 | 1.613 | 1.425 | 1.365 | 0.532 |
| 56 | Far C-18a | 5.536 | 0.364 | 2.068 | 1.372 | 1.270 | 1.191 | 0.635 |
| 65 | Far C-18a | 10.393 | 3.118 | 2.103 | 0.835 | 2.725 | 0.768 | 0.840 |
| 121 | Far C-18a | 5.084 | 0.549 | 2.145 | 0.941 | 1.845 | 0.278 | 0.111 |
| Average ± Standard Deviation | | 7.220 ± 2.441 | 1.432 ± 1.269 | 1.831 ± 0.549 | **1.190 ± 0.365** | 1.816 ± 0.653 | 0.900 ± 0.485 | 0.529 ± 0.307 |
| 147 | Iceberg Alley | 2.873 | 1.104 | 0.713 | 0.272 | 0.374 | 0.291 | 0.319 |
| 154 | Iceberg Alley | 2.787 | 0.402 | 1.274 | 0.274 | 0.442 | 0.227 | 0.258 |
| Average ± Standard Deviation | | **2.830 ± 0.061** | 0.753 ± 0.496 | 0.993 ± 0.396 | **0.273 ± 0.002** | **0.408 ± 0.049** | 0.259 ± 0.045 | 0.289 ± 0.043 |
| 141 | Control Station | 9.630 | 1.878 | 0.996 | 2.152 | 3.099 | 0.747 | 1.089 |
| 170 | Control Station | 4.030 | 0.358 | 0.718 | 0.958 | 1.732 | 0.435 | 0.314 |
| Average ± Standard Deviation | | 6.830 ± 3.960 | 1.118 ± 1.075 | 0.857 ± 0.197 | **1.555 ± 0.844** | 2.415 ± 0.967 | **0.591 ± 0.221** | 0.702 ± 0.548 |

this issue). These results imply that the iceberg presence in western Powell Basin waters decreased the overall biomass, particularly of nanoplankton cells, both as chla concentration and cell counts, but affects composition selecting for growth of large cells.

Waters at Iceberg Alley were colder, with less dissolved oxygen and higher transparency associated with less total chla and phaeopigments, less chla at all size fractions, with the exception of picoplankton ( < 3 μm), less phaeopigments in the nanoplankton fraction (3-10 μm), lower primary production and particulate carbon and nitrogen, lower $NH_4^+$ and lower photosynthetic efficiency (Fv/Fm) than at Close C-18a. This indicates an area with similar chla size structure as the C-18a area, but with less abundant and less healthy phytoplankton (Tables 1–4, Figs. 2 to 4).

Stations close to C-18a (Fig. 5A) and at Iceberg Alley (Fig. 5B) had similar cell size distribution within the 0-100 m surface layer, with smaller cells dominating the biomass. The main difference

**Table 3**
Dissolved inorganic nutrients and particulate organic carbon and nitrogen. Data represent the average values in the top 100 m, and the mean and one standard deviation from the mean for each location are summarized beneath each sampling region. Locations that are significantly different from Close C-18a are marked in bold ($\alpha=0.05$) and in bold italics ($\alpha=0.1$). Number of samples in top 100 m was 6-8 depths.

| Event | Sampling Region | Phosphate (m mol $m^{-2}$) | Nitrite (m mol $m^{-2}$) | Ammonium (m mol $m^{-2}$) | Silicate (m mol $m^{-2}$) | Nitrate (m mol $m^{-2}$) | Particulate Organic Carbon(mg $m^{-2}$) | Particulate Organic Nitrogen(mg $m^{-2}$) |
|---|---|---|---|---|---|---|---|---|
| 3 | Close C-18a | 202.1 | 12.7 | 73.9 | 7580.6 | 2961.8 | - | - |
| 29 | Close C-18a | 184.4 | 19.2 | 84.4 | 6199.4 | 2928.2 | 6755.1 | 1191.1 |
| 39 | Close C-18a | 188.3 | 17.1 | 101.9 | 6416.0 | 2834.7 | - | - |
| 101 | Close C-18a | 190.5 | 18.7 | 57.9 | 6756.7 | 2958.2 | 3257.3 | 789.9 |
| 108 | Close C-18a | 186.8 | 19.9 | 82.3 | 6268.7 | 2774.5 | 4468.3 | 1050.1 |
| Average ± Standard Deviation | | 190.5 ± 6.9 | 17.5 ± 2.9 | 80.1 ± 16.1 | 6644.3 ± 565.8 | 2891.5 ± 83.1 | 4826.9 ± 1776.2 | 1010.4 ± 203.5 |
| 8 | Far C-18a | 187.7 | 15.3 | 100.5 | 6938.6 | 2774.6 | - | - |
| 46 | Far C-18a | 179.7 | 19.1 | 96.0 | 5825.6 | 2649.2 | 3886.7 | 789.5 |
| 56 | Far C-18a | 187.7 | 17.4 | 79.8 | 6429.3 | 2730.8 | 4043.4 | 884.6 |
| 65 | Far C-18a | 186.7 | 18.6 | 80.5 | 6637.0 | 2826.5 | - | - |
| 121 | Far C-18a | 187.6 | 20.0 | 89.8 | 6160.4 | 2754.6 | 4438.6 | 1003.5 |
| Average ± Standard Deviation | | 185.9 ± 3.5 | 18.1 ± 1.8 | 89.3 ± 9.2 | 6398.2 ± 428.5 | **2747.2 ± 65.1** | 4122.9 ± 284.4 | 892.5 ± 107.2 |
| 147 | Iceberg Alley | 198.1 | 18.2 | 58.4 | 6974.8 | 2937.2 | 2495.0 | 593.0 |
| 154 | Iceberg Alley | 188.9 | 16.0 | 57.0 | 7398.7 | 3024.9 | 3066.0 | 698.5 |
| Average ± Standard Deviation | | 193.5 ± 6.5 | 17.1 ± 1.6 | ***57.7 ± 1.0*** | 7186.7 ± 299.8 | 2981.1 ± 62.0 | ***2780.5 ± 403.8*** | ***645.7 ± 74.6*** |
| 141 | Control Station | 179.5 | 18.8 | 81.9 | 6669.1 | 2737.2 | 5275.6 | 1097.9 |
| 170 | Control Station | 235.3 | 24.2 | 109.7 | 8235.4 | 3361.3 | 5630.2 | 1269.2 |
| Average ± Standard Deviation | | 207.4 ± 39.5 | 21.5 ± 3.8 | 95.8 ± 19.7 | 7452.3 ± 1107.5 | 3049.2 ± 441.3 | 5452.9 ± 250.7 | 1183.5 ± 121.2 |

was the lower overall biomass at Iceberg Alley. The size distribution at these sites was described by a negative exponential curve. In general, more small cells were seen at Far C-18a, 18 km away. In contrast, nanoplankton (5-10 μm) dominated at the Control Station (Fig. 5C) with minimum contribution by the smaller and larger size fractions.

Further analysis of the influence of the iceberg on chla distribution was determined by analyzing samples at 5 distances from the iceberg (Fig. 6). Surface chla showed higher concentration at 2 km ($p<0.05$), a distance not sampled with CTDs. The difference was significant with respect to 0.4 km and 18 km. Integrated chla (0-300 m) showed the same pattern as surface chla, but to a lesser degree ($p=0.245$).

Primary Production showed intermediate values (Fig. 7), with a range between 369 and 65 mg C $m^{-2}$ $d^{-1}$ within the euphotic zone (Table 4). Rates were highest close to C-18a and at the Control Station and lower 18 km away (Far C-18a). Lowest rates were measured at the Iceberg Alley stations. Rates are mainly related to chla concentrations, as expected for Antarctic coastal waters (Dierssen et al., 2000; Vernet et al., 2008), although values were higher than expected in waters close to the iceberg. For each location primary productivity variability was high; differences between Close and Far C-18a were not significant. The efficiency of carbon uptake ($P^B$), calculated as integrated production per integrated biomass during daylight hours at this time of the year was significantly higher close to the iceberg than 18 km away ($p=0.05$, Table 4).

## 4. Discussion

C-18a was sampled during austral fall of 2009, from mid March to mid April. Sun angle is low at this time of year at this latitude, and day length is also short (~12 h). A surface mixed layer with relatively warm and fresh waters was always present (35.5 ± 13.1 m). Winter water, represented by a temperature minimum, was located at ~100 m depth (Carmack and Foster, 1977). This layer was thicker and colder closer to the iceberg (Stephenson et al., this issue). Underneath this feature were the main thermocline and the Upper Circumpolar Deep Water. In general, coastal waters offer less stratification than waters in the central Weddell Sea (Gordon, 1998).

The western Powell Basin is a region often visited by free-floating icebergs. Tracks indicate a general drift North East along the continental slope of western Weddell Sea (Gladstone et al., 2001). C-18a followed the bottom topography, moving parallel to the continental slope (1600-3650 m depth; Fig. 1). We expected waters of the Iceberg Alley area, in the SW Powell Basin, to be the most affected by icebergs due to the seasonal drift of icebergs along the region as well as the combined effect of many small icebergs at the time of sampling. The C-18a area had also a seasonal signal but with only one iceberg present for 20 days (10-30 March 2009) the cumulative effect on the surrounding phytoplankton was thought to be less. Finally, the Control Station was considered the least influenced by icebergs.

The hydrography at the time of sampling is expected to be influenced by the icebergs present through the austral summer months, after sea ice retreat. The observed temperature gradient in the surface waters (0-100 m; Table 1) is in agreement with expected input by melting icebergs. Temperature-Salinity (T-S) diagrams show varying surface melting, from higher temperature and salinity at the Control Station east of C-18a, intermediate in the west (C-18a region), and minimum at the Iceberg Alley (Stephenson et al., this issue). Thus, far-field differences between C-18a waters and the Control Station water can be attributed to the presence of the iceberg C-18a. Near-field differences introduced by the iceberg at the time of sampling can be established by comparing Close C-18a and Far C-18a waters, 18 km away. Regional iceberg influence can be established from properties observed at Iceberg Alley.

The distribution of phytoplankton abundance along the meltwater gradient established by water temperature was opposite to our expectations (Table 2). The higher chla concentration observed at the Control Station and lower at Close C-18a and Iceberg Alley was in opposition to previous results (Smith et al., 2007; Schwarz and Schodlok, 2009). Different from large icebergs in the Ross Sea Ice Shelf (Arrigo et al., 2002; Rhodes et al., 2009), small free-drifting icebergs increase phytoplankton concentration

Please cite this article as: Vernet, M., et al., Impacts on phytoplankton dynamics by free-drifting icebergs in the NW Weddell Sea. Deep-Sea Research II (2011), doi:10.1016/j.dsr2.2010.11.022

**Table 4**
Primary productivity, fluorescence induction (FIRe) parameters and cell counts from flow cytometry data. Abbreviations include $Z_{eu}$ (euphotic zone depth), $P^B$ (efficiency of carbon uptake) and Phyto (phytoplankton). Production and fluorescence parameters represent the integrated (Primary Production and $P^B$) or average (Fv/Fm, $\sigma$, $\tau$) within the euphotic zone and the average of the top 100 m for the phytoplankton cell counts ($n$=number of cells). Fv/Fm is the maximum quantum efficiency of Photosystem II, in the dark; $\sigma$ is the functional absorption cross section of PSII; $\tau$ is the rate of electron transport of PSII (PQ re-oxidation). The mean and one standard deviation from that mean for each location are summarized beneath each sampling region. Locations that are significantly different from Close C-18a are marked in bold ($\alpha$=0.05) and in bold italics ($\alpha$=0.1). Number of samples in top 100 m was 6–8 depths.

| Event | Sampling Region | $Z_{eu}$ (m) | Primary Production (mg C $m^{-2}$ $d^{-1}$) | $P^B$ (mgC (mg Chla)$^{-1}$ $h^{-1}$) | Fv/Fm | $\sigma$ (Å$^2$ $q^{-1}$) | $\tau$ (μs) | Total Phyto ($n$∗$10^8$ $m^{-3}$) | Phyto > 10 μ ($n$∗$10^8$ $m^{-3}$) | Phyto 3–10 μ ($n$∗$10^8$ $m^{-3}$) | Phyto < 3 μ ($n$∗$10^8$ $m^{-3}$) |
|---|---|---|---|---|---|---|---|---|---|---|---|
| 3 | Close C-18a | – | – | – | – | | – | 27.67 ± 17.82 | 0.3657 ± 0.2909 | 12.04 ± 6.084 | 15.27 ± 12.06 |
| 29 | Close C-18a | 102 | 367.3 | 13.53 | 0.586 ± 0.060 | 931 ± 87 | 2418 ± 829 | 27.40 ± 13.93 | 0.4750 ± 0.2167 | 11.60 ± 4.714 | 15.33 ± 9.113 |
| 39 | Close C-18a | 110 | 368.9 | 14.05 | 0.614 ± 0.053 | 751 ± 123 | 3164 ± 355 | 31.97 ± 11.85 | 0.4075 ± 0.2982 | 20.18 ± 3.447 | 11.39 ± 9.145 |
| 101 | Close C-18a | 68 | 108.3 | 5.45 | 0.589 ± 0.040 | 579 ± 115 | 1454 ± 845 | 13.81 ± 6.028 | 0.3225 ± 0.1748 | 5.915 ± 1.810 | 7.570 ± 4.152 |
| 108 | Close C-18a | 70 | 258.2 | 8.44 | 0.639 ± 0.040 | 596 ± 98 | 2745 ± 380 | 29.09 ± 17.76 | 0.5314 ± 0.3452 | 12.06 ± 6.193 | 16.50 ± 11.19 |
| Average ± Standard Deviation | | | 275.7 ± 123.1 | 10.37 ± 4.14 | 0.607 ± 0.025 | 714 ± 164 | 2445 ± 728 | 25.99 ± 7.046 | 0.4204 ± 0.0837 | 12.36 ± 5.084 | 13.21 ± 3.697 |
| 8 | Far C-18a | 75 | 114.3 | 4.21 | 0.505 ± 0.029 | 601 ± 88 | 3442 ± 1522 | - | - | - | - |
| 46 | Far C-18a | 53 | 274.2 | 8.13 | 0.604 ± 0.070 | 727 ± 108 | 2595 ± 389 | 35.45 ± 21.52 | 0.5600 ± 0.3295 | 15.68 ± 8.867 | 19.22 ± 12.46 |
| 56 | Far C-18a | 50 | 234.7 | 7.87 | 0.626 ± 0.049 | 538 ± 19 | 2591 ± 224 | 30.52 ± 17.72 | 0.6350 ± 0.3127 | 9.245 ± 4.520 | 20.64 ± 13.02 |
| 65 | Far C-18a | - | - | - | 0.662 ± 0.020 | 509 ± 57 | 3809 ± 900 | 31.63 ± 15.24 | 0.5943 ± 0.3586 | 11.54 ± 3.623 | 19.49 ± 11.39 |
| 121 | Far C-18a | 34 | 106.4 | 3.13 | 0.589 ± 0.022 | 595 ± 96 | 2995 ± 294 | 21.38 ± 9.819 | 0.5244 ± 0.3325 | 10.39 ± 4.110 | 10.47 ± 5.839 |
| Average ± Standard Deviation | | | 182.4 ± 84.8 | 4.67 ± 3.41 | 0.597 ± 0.059 | 594 ± 84 | 3086 ± 535 | 29.75 ± 5.963 | ***0.5784 ± 0.0047*** | 11.71 ± 2.803 | 17.45 ± 4.697 |
| 147 | Iceberg Alley | 53 | 64.5 | 5.46 | 0.567 ± 0.048 | 885 ± 165 | 3309 ± 921 | 21.12 ± 9.304 | 0.2425 ± 0.1859 | 13.46 ± 4.960 | 7.425 ± 4.982 |
| 154 | Iceberg Alley | 55 | 86.9 | 6.77 | 0.573 ± 0.041 | 727 ± 149 | 3878 ± 808 | 22.91 ± 11.89 | 0.2400 ± 0.1690 | 14.64 ± 6.360 | 8.028 ± 5.824 |
| Average ± Standard Deviation | | | ***75.5 ± 15.8*** | 6.11 ± 0.93 | ***0.570 ± 0.004*** | 806 ± 111 | 3594 ± 402 | 22.02 ± 1.262 | **0.2413 ± 0.002** | 14.05 ± .0.838 | 7.726 ± 0.426 |
| 141 | Control Station | 54 | 255.4 | 7.57 | 0.399 ± 0.063 | 832 ± 89 | 3354 ± 593 | 44.52 ± 18.66 | 1.823 ± 0.8645 | 18.39 ± 6.927 | 24.31 ± 11.01 |
| 170 | Control Station | 58 | 232.8 | 7.21 | 0.374 ± 0.038 | 1021 ± 204 | 3990 ± 640 | 37.06 ± 14.18 | 2.089 ± 0.9024 | 10.43 ± 2.929 | 24.54 ± 11.02 |
| Average ± Standard Deviation | | | 244.1 ± 16.0 | 7.39 ± 0.25 | **0.386 ± 0.018** | 927 ± 133 | 3672 ± 450 | **40.76 ± 5.274** | **1.956 ± 0.0188** | 14.41 ± 5.626 | **24.42 ± 0.0164** |

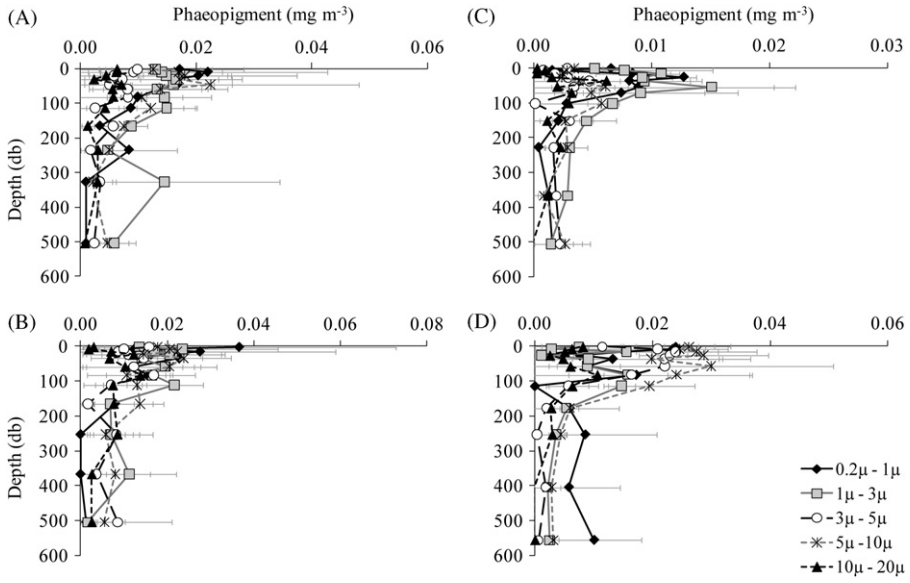


**Fig. 3.** Phaeopigment profiles for each size fraction at the Close C-18a stations (A), Far C-18a stations (B), the Iceberg Alley stations (C) and the Control Stations (D). Data represents the average of all stations at a given location, and error bars represent one standard deviation from the mean. Data is plotted at the average depth for the location. Note different pigment scales for the different areas.

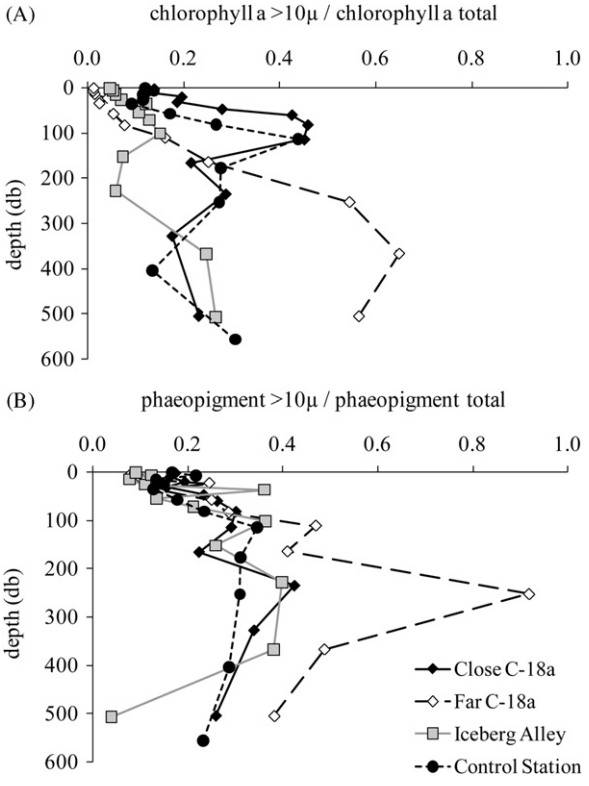


**Fig. 4.** Profiles of chlorophyll *a* (A) and phaeopigments (B) in the greater than 10 μm fraction as a function of the total chlorophyll (or phaeopigments). Data represents the average of all stations at a given location.

and favor diatoms, known to be selected by krill as favorite food (Ross et al., 2000). Although the chla accumulation around grounded icebergs (Whitaker, 1977) is not observed around free-floating icebergs, the latter drift when in open waters, distributing their influence over large areas in short periods of time (Bigg et al., 1997). The accumulated effect could be in the order of thousands of km$^2$ per month for an iceberg of the dimensions of C-18a (Helly et al., this issue).

High variability in the response of phytoplankton abundance to icebergs has been observed in previous studies. An iceberg might be expected to decrease or increase chla concentration and this difference might be related to *in situ* chla concentrations (Schwarz and Schodlok, 2009). These authors found that if chla $<0.36$ mg m$^{-3}$ the iceberg tended to increase surface chla after its passage while levels tended to decrease when *in situ* chl a concentrations were $>0.6$ mg m$^{-3}$. Average chla abundance in surface waters of western Powell Basin during fall 2009 was on the order of 0.55 mg m$^{-3}$ (Fig. 2B) and decreased to an average 0.45 mg m$^{-3}$ (Fig. 2A) at $<1$ km from C-18a. However, at 2 km away the chla increased significantly ($p<0.05$) to a concentration $\sim$11% higher 16-18 km away (Fig. 6A). Schwarz and Schodlok (2009) also found variability in the chla response at different times of the year, with no increase during October, February and March and positive increase in November, January and February. Due to the expected variability introduced by the iceberg, we consider our results an underestimation of the patterns and processes generated by the iceberg. Sampling an iceberg was challenging as the iceberg drifted, traveling over different waters along the way. Repetitive sampling within a 3-week period, as on this cruise, was done in different water masses which increases variance and decreases signal to noise ratio for the variables of interest. The icebergs' high-frequency motion, (rotation and surging) added variability as well. Large calving events might be less frequent and variable in magnitude, but sides of the icebergs fell frequently creating "growlers" and brash that introduced surface patchiness (Robe, 1978). The size of the iceberg can limit optimum sampling: a large proportion of time can be spent changing location. The threat of calving limits the distance where the ship can operate safely and sampling of waters a few meters away from the iceberg can only be done remotely. Iceberg drift could be another source of variability when determining an iceberg's dynamics and its effect on the surrounding ecosystem. C-18a drifted at an average speed of 0.15-0.52 km h$^{-1}$ (Helly et al., this issue), which was slow compared to A52, that was moving at a speed of 1.45 km h$^{-1}$ in December 2005 off Clarence Island (Smith et al., 2007), but similar to the mean daily iceberg drift of $11.5\pm7.2$ km d$^{-1}$ ($\sim$0.5 km h$^{-1}$; Schodlok et al., 2006).

Please cite this article as: Vernet, M., et al., Impacts on phytoplankton dynamics by free-drifting icebergs in the NW Weddell Sea. Deep-Sea Research II (2011), doi:10.1016/j.dsr2.2010.11.022

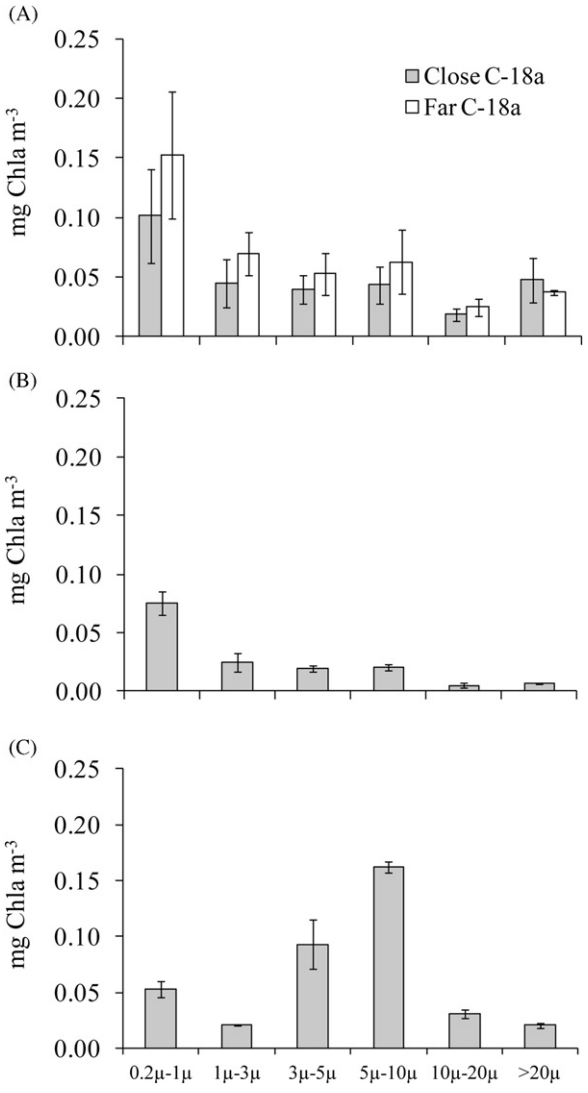


**Fig. 5.** One hundred (100)-m averaged chlorophyll a for each size fraction, at the Close and Far C-18a stations (A), the Iceberg Alley stations (B) and the Control Station (C). Data represents the average of all stations at a given location and error bars represent one standard deviation from the mean. Six to eight depths were sampled per CTD cast.

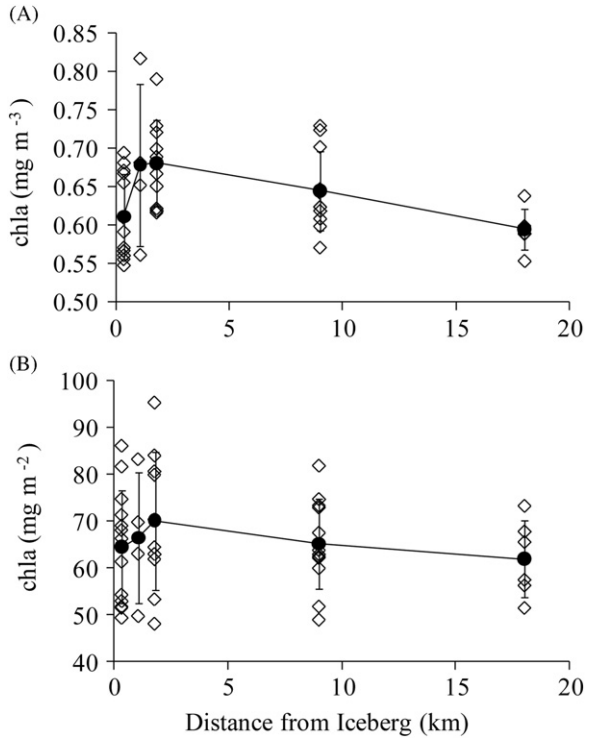


**Fig. 6.** Chlorophyll a calculated from the MOCNESS CTD fluorometer, plotted as a function of distance from the C-18a iceberg. Open diamonds represent the average value of the top 10 m of each trawl (A) or the average chlorophyll a integrated to 300 m for each trawl (B); filled circles in both panels represent the average of all trawls for a given location. Error bars represent one standard deviation from the mean. The similarity in variances was tested with Levine's test for multiple samples of unequal size and with non-normal distribution, $p=0.245$. Non-parametric comparison of means (Mann-Whitney test) indicate chla concentration near the surface (0-10 m) at 2 km is significantly higher than at 18 km ($p<0.05$).

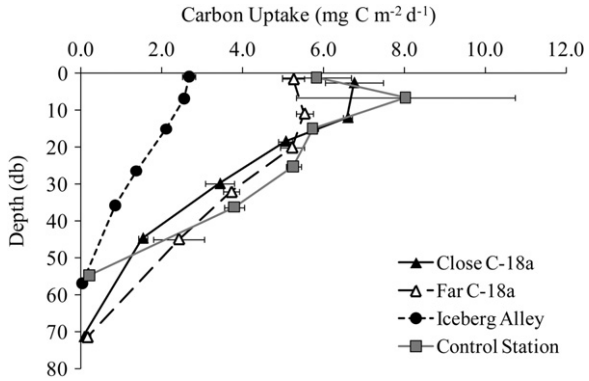


**Fig. 7.** Profiles of Primary Production at each of the sampling locations. Depths of incubation correspond to 100%, 50%, 25%, 10%, 5% and 1% of the surface irradiance. Data represent the average of all stations at a given location; error bars represent one standard deviation from the mean. Data are plotted at the average depth sampled for each bottle at each location.

C-18a drift generated a wake behind the iceberg (towards the South West) observed during surface mapping (Helly et al., this issue). Lower chla concentrations were observed $<5$ km, increasing farther out (5-18 km). The wake had a permanence in excess of 10 days measured from the corresponding residence time of the surface features (Helly et al., this issue), similar to the 6 days in Schwarz and Schodlok (2009). The phytoplankton growth needed to account for the observed 30% increase in chla after 10 days is within the rates expected for healthy Antarctic phytoplankton. While cell doubling of 2 days is considered maximum at 0 °C (Eppley, 1972), average growth in the euphotic zone can vary from 0.2 to 0.4 $d^{-1}$ for phytoplankton with abundant nutrients at the height of the growth season in January (Garibotti et al., 2003b). Our results support the notion of healthy phytoplankton in the iceberg's vicinity, indicated by high variable fluorescence and $P^B$ (Table 4). Preliminary growth estimates, based on primary production and total suspended particulate carbon (Tables 3 and 4) provide an average rate within the mixed layer (0-~40 m) of $0.07 \pm 0.02$ $d^{-1}$ or a division every ~14 days, sufficient to account for the observed increase in chla.

### 4.1. Patterns of phytoplankton distribution around the iceberg

Three patterns in chla distribution were analyzed in this study with respect to the iceberg's influence: surface chla (Fig. 6A), integrated chla in the euphotic zone (Fig. 6B) and chla size distribution with depth and distance from iceberg (Figs. 4 and 5). Results are mixed when compared with previous results, with phytoplankton biomass lower at the iceberg than expected (Table 2A). Similarly, primary production was low close to the iceberg (Table 4). In contrast, physiological parameters

Please cite this article as: Vernet, M., et al., Impacts on phytoplankton dynamics by free-drifting icebergs in the NW Weddell Sea. Deep-Sea Research II (2011), doi:10.1016/j.dsr2.2010.11.022

indicated a healthy community with higher $P^B$ <1 km from C-18a than at 18 km away and high variable fluorescence (Fv/Fm) (Table 4).

The pattern of surface chla distribution described for the December 2005 icebergs (Smith et al., 2007) was observed in waters around C-18a, with chla significantly higher at a distance of 2 km (Fig. 6A). Here we show that this pattern extends to depth (Fig. 6B). However, chla biomass was on average lower than expected at the iceberg's proximity (Table 2B), higher in control areas (Far C-18a and the Control Station) and lowest at Iceberg Alley. Thus, the gradient in phytoplankton biomass between stations was opposite to meltwater input, lowest at Iceberg Alley and Close C-18a, and highest at Far C-18a and the Control Station.

Large phytoplankton cells (chla >10 μm) were more abundant near C-18a compared to 18 km away and the Control Station (Figs. 2A and 4A) with a peak at 70-100 m, in agreement with findings that diatoms, mostly large nano- or microphytoplankton, dominated phytoplankton composition near the iceberg (Cefarelli et al., this issue). *Corethron pennatum* and various *Chaetoceros* spp. were abundant microplanktonic species while *Thalassiosira* and *Fragilariopsis nana* contributed to the nanoplankton. Large phytoplankton cells are commonly associated with productive areas in the Weddell Sea (Fryxell, 1989; Kang and Fryxell, 1993). Diatoms in long chains and colonial prymnesiophytes with mucilagineous colonies are found at the ice edge in the spring, as well as at oceanic fronts (Kang et al., 2001; Krell et al., 2005). In contrast, small nanoplanktonic flagellates dominate areas of lower productivity (Fryxell, 1989; Kang and Fryxell, 1993). This is a general pattern of cell size distribution and composition in relation to productivity found elsewhere in Antarctica (Kang and Lee, 1995; Figueiras et al., 1998; Gall et al., 2001; Varela et al., 2002).

Chla size distribution showed a notable variability with respect to iceberg-impacted and non-impacted areas (Fig. 5). Cell size distribution in phytoplankton describes structure within the pelagic ecosystem (Chisholm, 1992; Ehnert and McRoy, 2007; Hewes, 2009); it is maintained by differential productivity (Fiala et al., 1998; Trembley and Legendre, 1994). It has been proposed that large cells can be controlled by bottom-up (physical and/or chemical) processes while nano- and picoplankton cells (<10 μm) respond to grazing pressure, e.g. microzooplankton grazing (Smith and Lancelot, 2004). Different grazers can also affect phytoplankton community composition as some grazers specialize on microphytoplankton (i.e. *Euphausia superba* or Antarctic krill) and salps feed mainly on smaller cells (<10 μm, *Salpa thompsonii*) (Walsh et al., 2001). The variability in chla size distribution observed can be used to infer the type of grazers in the studied areas and the effect that the iceberg(s) can have on phytoplankton through grazing pressure (Kawaguchi et al., 2000). The presence of large cells (>10 μm) close to the iceberg (Fig. 5A) is expected to sustain macrograzers. In contrast, the waters in the Control Station dominated by nanoplankton (Fig. 5C) and impoverished in large cells, would maintain microzooplankton or salps (Dubischar and Bathmann, 1997).

Similar to chla distribution, primary production was lower close to the iceberg and higher at Control Station (Table 4). Biomass specific primary production or $P^B$ had the opposite pattern indicating production was limited by biomass. Primary production in coastal polar waters is explained mostly by chla abundance (~70%, Dierssen et al., 2000). Early measurements have shown high production over the shelf (0.41 g C $m^{-2}$ $d^{-1}$) and lower in deep waters (0.104 g C $m^{-2}$ $d^{-1}$) (El Sayed and Taguchi, 1981; Longhurst, 1998; Smith and Nelson, 1990). While winter production can be very low (0.1 mg C $m^{-2}$ $d^{-1}$), summer ice-edge communities in the Weddell Sea can produce up to 2.4 g C $m^{-2}$ $d^{-1}$ (Park et al., 1999). Overall the primary production estimates in the fall of 2009 were average for the coastal waters of the Weddell Sea and not as high as those from ice-edge communities.

Combining observed primary production rates with C:N ratio of 5.4, a C:Chla ratio of 136 (Tables 2A and 3) and a high proportion of sedimenting cells (Smith et al., this issue), compared to a C:Chla ratio of 72 in summer (Garibotti et al., 2003b) and a C:N of 4.5 for healthy cultures, we deduce that the phytoplankton encountered in Powell Basin represents a typical fall community, rich in carbon but healthily growing. Whether the *in situ* growth can translate to chla accumulation will depend on, among other factors, loss terms. As shown above (Section 4) *in situ* growth rates can explain a 30% increase in biomass after the iceberg's passage. We propose here that the iceberg influence can promote phytoplankton losses and that chla accumulation will occur only where the growth enhanced by turbulent mixing and Fe addition can counteract any large loss rates.

### 4.2. Physical, chemical and biological processes related to the iceberg

Three main oceanic processes are considered to explain the phytoplankton patterns observed. They are unique to the iceberg, originating from the ice or created through the iceberg's presence in sea water. Each process is known to facilitate growth but can also create losses. First, the melting of the iceberg is driven by three main mechanisms related to basal melting and melting on the sides of the iceberg. Changes in chla could originate from increased mixing introduced by the iceberg as well as nutrient enrichment, as seen by increased dissolved nitrate and dissolved iron. Biologically, the presence of zooplankton can affect phytoplankton abundance via grazing and nutrient release. Each of these processes is discussed below.

#### 4.2.1. Melting and turbulence introduced by the iceberg

Three main physical processes originating from the iceberg's melting and movement were observed during Iceberg III cruise in 2009 (Stephenson et al., this issue; Helly et al., this issue). Seawater is warmer than ice, melting the iceberg's outer surface. The first process refers to melting at the base of the iceberg, or basal melting (Donaldson, 1978; Jenkins, 1999). The effects of this process, occurring between 50 and 200 m depth, would impact phytoplankton below the mixed layer, at the bottom of the euphotic zone. The end result is expected to be a dilution of phytoplankton concentration in waters close to the iceberg. The dilution could be due to the input of freshwater from the iceberg that lacks biological components. Alternatively, dilution could also occur from entrainment of deep seawater (>100 m) with lower phytoplankton concentration towards the surface (Fig. 4). In this process, the freshwater produced at 200 m in C-18a (the iceberg's bottom is considered to be between 150-192 m) was less dense and rose along the sides of the iceberg, mixing with the surrounding waters until reaching a level of same water density. The end result was colder and more saline water towards the surface. In a T-S diagram, a layer with saltier, colder water was seen above the layer of temperature minimum, or winter water (Stephenson et al., this issue). About 10 of the 65 CTDs taken during Iceberg III show this type of physical process. The lack of a more consistent observation of the melt-water saline layer could mean that the process was intermittent or that it was more obvious during certain iceberg positions or motions.

Another process would decrease phytoplankton concentration from surface to depth by advecting cells away from the iceberg's face; it is expected to be an important factor in lowering chla between 50 and 200 m depth. Chla profiles close to C-18a showed lower pigment concentrations in the 50-100 layer (Fig. 2A) with respect to farther away (Fig. 2B). The melting from the iceberg's

Please cite this article as: Vernet, M., et al., Impacts on phytoplankton dynamics by free-drifting icebergs in the NW Weddell Sea. Deep-Sea Research II (2011), doi:10.1016/j.dsr2.2010.11.022

flanks can result in two vertical layers of freshwater close to the iceberg, the inner one moving upwards and the outer one moving downwards (Neshyba, 1977). The turbulence mixes meltwater with the surrounding waters and moves freshwater away from the iceberg along an isopycnal slope or layer of diminishing density (Helly et al., this issue). This process was observed near C-18a as small, steplike changes in the salinity/density profile, and was present both above and below the winter water (Stephenson et al., this issue).

It is expected that freshwater input would dilute waters around the iceberg, decreasing phytoplankton concentration, particularly at the mixed layer. The melting of brash ice from iceberg calving probably decreased surface salinity and chla further (Robe, 1978). In this process a freshwater layer rises to the surface without any considerable mixing with surrounding waters (Donaldson, 1978; Neshyba, 1977). This water would be seen as fresher in the vicinity of the iceberg (Helly et al., this issue) during surface mapping. For C-18a, the fresher water was seen more clearly at the iceberg's wake and was persistent for 10 days.

Iceberg melting can also be related to the chla $>10\,\mu m$ within the mixed layer and the chla $>10\,\mu m$ observed at 70-100 m depth close to the iceberg (Fig. 4A). The upwards flow of water along the iceberg's side originating from basal melting called also "upwelling" by icebergs (Neshyba, 1977) can be equated to upwelling events in western boundary currents. Upward vertical motion has been correlated with increases in relative proportion of large cells (Rodriguez et al., 2001), as shown here (Fig. 4A). Abundance of diatoms is a well known phenomenon associated with upwelling events (i.e. Montero et al., 2007). The upward velocity associated with eddies and unstable fronts, 10-100 km in dimension, also promotes large cells. We propose here that upwelling by iceberg melting can have a similar effect on phytoplankton size distribution.

In summary, we expected that physical processes of underwater iceberg melting, combined with surface melting from calving and entrainment of deep water by the iceberg melting and displacement, to reduce phytoplankton abundance. In addition, these physical processes promote growth of large cells, known to dominate productive environments. These were indeed the patterns observed within 1-2 km from the iceberg (Fig. 6; Smith et al., 2007).

#### 4.2.2. *Icebergs as a source of nitrate and iron*

In addition to being a source of freshwater, icebergs are expected to release nutrients to the seawater. The increased dissolved nitrate concentration measured in the 0-100 m layer of seawater close to the iceberg ($<1$ km from the iceberg face) in relation to similar water 16-18 km away ($p<0.1$, Table 3), indicates that nitrate increases as the iceberg passes through a body of water. The nitrate enrichment was most pronounced in the 50-100 m layer ($p<0.05$). Three processes can be considered to produce this effect: decreased phytoplankton growth, entrainment of deep water from the main thermocline (below 150 m) or input from meltwater. As higher nitrate concentrations co-occur with lower phytoplankton abundance, accumulation of nitrate could originate from decreased nitrate uptake. Such reduction in nitrate would be related to a reduction in phosphate as well, as both nutrients are needed to support all phytoplankton, and this has not been observed. Similarly, if higher nitrate originates from enrichment of surface waters by entrainment of deep waters through mixing from meltwater (Jenkins, 1999) or by alteration of the water column structure as an iceberg with a 200-m keel passes through a 50-m mixed layer, we would expect to measure also higher phosphate and silicate. This was not observed either. Parker et al. (1978) mention a concentration gradient of nitrate away from the iceberg and conclude that icebergs are a source of dissolved inorganic nitrogen, similar to our observations. The melting of continental ice is considered a potential source of dissolved nitrate in the water column, originating from atmospheric deposition over the polar cap. Atmospheric Nitrogen (N) deposition occurs both in the Arctic (Hooper, 1971) and the Antarctic (Parker et al., 1978; Bauer, 1978). In Antarctica, the input of nitrate and ammonium ($NH_4^+$) to surface ocean waters is calculated as 1%-7% of the nitrate pool in the mixed layer of the Southern Ocean. Average concentration in the ice is $19.57\,mg\,m^{-3}$ nitrate and $13.34\,mg\,m^{-3}$ ammonium due to stratospheric ionization processes. Thus icebergs could contain about 7 times the concentration of nitrate of surface waters ($2.7\,mg\,m^{-3}$).

Input of Fe in the water column by sea ice melting in the spring is considered key to the production in the Ross Sea (Sedwick and DiTullio, 1997; Tagliabue and Arrigo, 2006). We can expect continental ice to bring Fe as well, both from minerals attached to the bottom of the iceberg (ice-drafted detritus) or from atmospheric input (Smith et al., 2007). This could be a process of micronutrient injection to the coastal current in Antarctica since icebergs, as predicted from modeling (Lancelot et al., 2009), are expected to remain in coastal waters (Gladstone et al., 2001). We had hypothesized that the iceberg was a source of dissolved Fe, able to stimulate phytoplankton growth in Fe-limited waters. de Baar (1995) measured higher dissolved Fe in the wake of an iceberg in the Polar Front. Terrigenous material from icebergs east of Clarence Island sampled in 2005 was able to maintain phytoplankton growth (Smith et al., 2007). Lin et al. (this issue) found higher dissolved Fe in waters of lower salinities within the Powell Basin. These samples originated from surface waters near the iceberg ($<1$ km) and were collected with metal-free sampling gear. They concluded that trends in the horizontal and vertical distributions of dissolved and particulate Fe suggested that Fe may be scavenged by abiotic and biotic processes near icebergs. Accumulation of diatoms close to the iceberg, as measured by microscopy (Cefarelli et al., this issue) and chla size fractions (Fig. 5), is consistent with an environment rich in Fe (Helbling et al., 1991; Holm-Hansen et al., 1994; Coale et al., 2004; Boyd et al., 2000). Furthermore, the high photosynthetic efficiency in phytoplankton impacted by icebergs, compared to those in the Control Station, are further indication of Fe-rich cells under the iceberg's influence (DiTullio et al., 2005; Hopkinson et al., 2007).

#### 4.2.3. *Grazing in the iceberg's vicinity*

Potential grazing from the observed zooplankton abundance and composition, and its variability with respect to iceberg-impacted and non-impacted waters, is in agreement with the distribution of phytoplankton in the different chla size fractions. The enrichment in large cells observed in the C-18a area and to a lesser extent at Iceberg Alley (Fig. 5A and B) suggests that iceberg waters can maintain grazers that select for large cells, such as the Antarctic krill *Euphausia superba* (Daniels et al., 2006). At the Control Station (Fig. 5C), nanoplankton can feed large protists or grazers that specialize in small cells, such as salps (Kawaguchi et al., 2000; Pakhomov et al., 2006). These results agree with zooplankton distribution at C-18a: macrozooplankton biomass was highest close to the iceberg (0.4 km), and diminished exponentially with distance (Kaufmann et al., this issue). There was higher total zooplankton biomass at 0.4 km from C-18a, declining to a minimum at 18 km away, with intermediate biomass at 9 km (Table 5). Composition of zooplankton also changed with distance to the iceberg: the highest proportion of large *E. superba* biomass

Please cite this article as: Vernet, M., et al., Impacts on phytoplankton dynamics by free-drifting icebergs in the NW Weddell Sea. Deep-Sea Research II (2011), doi:10.1016/j.dsr2.2010.11.022

**Table 5**
Zooplankton abundance in the Powell Basin in March-April 2009, as wet weight and number of individual per 1000 L, as a function of distance from the C-18a iceberg, the Control Station and Iceberg Alley. Temperature was used as an indicator of meltwater input. The relationship between biomass and numerical abundance is not 1:1 as krill juveniles dominated at the Control Station and adults at other locations (Kaufmann et al., this issue).

| | | Iceberg Alley | Close C-18a | - | - | Far C-18a | Control Station |
|---|---|---|---|---|---|---|---|
| | Distance from C-18a (km) | – | 0.37 | 1.85 | 9.26 | 18.52 | – |
| | Mixed Layer Temp (°C ± StDev) | −0.8784 ± 0.1121 | −0.1798 ± 0.2077 | – | – | 0.1964 ± 0.2658 | 0.1649 ± 0.1128 |
| | *N* | 12 | 9 | 8 | 6 | 6 | 4 |
| **Zooplankton Abundance** | | | | | | | |
| Weight/Volume | Mean | 95.12 | 305.40 | 195.47 | 97.96 | 22.09 | 27.51 |
| (g 1000 $m^{-3}$) | 95% CI | 58.30 | 334.64 | 187.88 | 63.73 | 10.52 | 13.60 |
| Number/Volume | Mean | 39.60 | 67.38 | 137.63 | 119.34 | 45.42 | 130.13 |
| (#1000 $m^{-3}$) | 95% CI | 13.75 | 63.94 | 101.30 | 48.23 | 20.90 | 117.04 |

was at 0.4 km from C-18a whereas the Control Station had the lowest. Highest salp biomass was within 2 km of the iceberg and dominant at the Control Station, although overall salp biomass was low. This small cell-salp vs. large cell-krill distribution is observed in Southern Ocean waters as a result of sea ice variability (Loeb et al., 1997) and increased influence of oceanic waters over the continental shelf (Quetin et al., 2007). Long-term changes in krill abundance are attributed to changes in size distribution of the food source (Atkinson et al., 2004). Similar to other oceanographic features, an iceberg creates high variability in food availability and is proposed here that it can support high grazer biomass.

Phaeopigments are a by-product of chla degradation by grazing and suspended phaeopigments can be indicative of microzooplankton grazing (Lorenzen, 1967; Welschmeyer and Lorenzen, 1985). Assuming similar photodegradation rates for suspended phaeopigments, Far C-18a and the Control Station had higher microzooplankton grazing than waters close to the iceberg (Table 2B, Fig. 3). Thus, large phytoplankton and krill grazing prevailed close to C-18a while microzooplankton grazing and nanoplankton cells were more prominent in waters not affected by icebergs.

If we assume that fall phytoplankton will have been subjected to heavy grazing pressure during the previous growth season, the distribution at the Control Station can be considered the average at this time of year. Krill had grazed down the diatoms and only smaller cells remain (Walsh et al., 2001; Hegseth and Von Quillfeldt, 2002; Garibotti et al., 2003b; Froneman et al., 2004), a condition labeled post-bloom (Hernandez-Leon et al., 2008). That waters affected by icebergs remain rich in diatoms late in the season can be attributed to the beneficial effect that icebergs can have over phytoplankton community composition, cell physiology and production efficiency, as described in this paper. That icebergs sustain a large grazer population can be estimated by comparing macrozooplankton volume to chla concentration at each location (Tables 2 and 5): this proportion is an order of magnitude higher at Close C-18a and Iceberg Alley than at Far C-18a and the Control Station. High $NH_4^+$ concentrations $<1$ km from the iceberg, produced from zooplankton metabolism, can be attributed to high grazing pressure as well.

## 5. Conclusions - The Iceberg Ecosystem

The phytoplankton distribution in relation to C-18a and other icebergs can be explained within the unique pelagic ecosystem associated with free-floating icebergs. We have shown that phytoplankton close to icebergs is healthy, as expected from nutrient-rich environments, and actively growing. The community composition is characteristic of productive areas: rich in large cells. Chla increased 10 days after the iceberg's passage (Helly et al., this issue) and the accumulation can be accounted for by the growth rate obtained from this study. Why doesn't chla accumulate close to C-18a? We propose that during March-April 2009, in the austral fall, the loss of phytoplankton biomass at the iceberg's vicinity was larger than growth. Both physical and biological processes decreased phytoplankton biomass. The low temperature at Iceberg Alley and Close C-18a indicated meltwater input, diluting phytoplankton. The mixing, vertical upward movement and nutrient enrichment all contribute to healthy cells. In addition, zooplankton distribution had the opposite pattern to chla, highest $<1$ km from C-18a and lowest at the Control Station, and the proportion of zooplankton biomass to phytoplankton was an order of magnitude higher close to the iceberg. High sedimentation rates associated with C-18a (Smith et al., this issue; Shaw et al., this issue) is consistent with grazers associated to iceberg(s) and an activation of the food chain by the iceberg community. Iceberg Alley is similar to Close C-18a in composition but further along in the seasonal development, with zooplankton having grazed down phytoplankton to winter levels. The system is one of top down control of phytoplankton close to the iceberg. The zooplankton community is associated exclusively with the iceberg(s), such that phytoplankton can accumulate in waters left behind by the iceberg's passage.

## Acknowledgments

The authors thank Wendy Kozlowski and Lynn Yarmey for invaluable contributions in data analysis and manuscript preparation; to Dr. Ronald Kaufmann for MOCNESS data; Mr. Mattias Cape and Dr. Corine Gle for figure preparation and revising the manuscript; J.J. MacIsaac Facility for Aquatic Cytometry at Bigelow Laboratory for Ocean Sciences for flow cytometer analysis; co-Principal investigators and collaborators in this project in particular Drs. John Helly, Ronald Kaufmann, Alison Murray and Mr. Gordon Stephenson for invaluable discussions. The authors gratefully acknowledge the support of Raytheon Polar Services for logistical support in the field and to the Captain and crew of the A.S.V. *Nathaniel B. Palmer*. Fig. 1 was made using Ocean Data View (R. Schlitzer, http://odv/awi.de, 2010). This project was funded by NSF award ANT-0636730 to M. Vernet and the NSF support is gratefully acknowledged.

## References

Armstrong, F.A.J., Stearns, C.R., Strickland, J.D.H., 1967. The measurement of upwelling and subsequent biological processes by means of the Technicon AutoAnalyzer and associated equipment. Deep-Sea Research 14, 381–389.

Arrigo, K.R., van Dijken, G.L., Ainley, D.G., Fahnestock, M.A., Markus, T., 2002. Ecological impact of a large Antarctic iceberg. Geophysical Research Letters 29, 7.

Atkinson, A., Siegel, V., Pakhomov, E., Rothery, P., 2004. Long-term decline in krill stock and increase in salps within the Southern Ocean. Nature 432, 100–103.

Atlas, E.L., Gordon, L.I., Hager, S.W., Park, P.K., 1971. A practical manual for the use of the Technicon Autoanalyzer in seawater nutrient analyses, rev. Technical Report 71-22. Oregon State University, Department of Oceanography, Corvallis.

Bauer, E., 1978. Non-biogenic fixed nitrogen in Antarctic surface waters. Nature 276 (2), 96.

Bernhardt, H., Wilhelms, A., 1967. The Continuous determination of low level iron, soluble phosphate and total phosphate with the autoanalyzer. Technicon Symposium: Automation in Analytical Chemistry, vol. 1, pp. 385–389.

Bigg, G.R., Wadley, M.R., Stevens, D.P., Johnson, J.A., 1997. Modelling the dynamics and thermodynamics of icebergs. Cold Regions Science and Technology 26, 113–135.

Boyd, P.W., Watson, A.J., Law, C.S., Abraham, E.R., Trull, T., Murdoch, R., Bakker, D.C.E., Bowie, A.R., Buesseler, K.O., Chang, H., Charette, M., Croot, P., Downing, K., Frew, R., Gall, M., Hadfield, M., Hall, J., Harvey, M., Jameson, G., LaRoche, J., Liddicoat, M., Ling, R., Maldonado, M.T., McKay, R.M., Nodder, S., Pickmere, S., Pridmore, R., Rintoul, S., Safi, K., Sutton, P., Strzepek, R., Tanneberger, K., Turner, S., Waite, A., Zeldis, J., 2000. A mesoscale phytoplankton bloom in the polar Southern Ocean stimulated by iron fertilization. Nature 407, 695–702.

Carmack, E.C., Foster, T.D., 1977. Water masses and circulation in the Weddell Sea. In: Dunbar, M.J. (Ed.), Polar Oceans, pp. 151–165.

Carrillo, C.J., Karl, D.M., 1999. Dissolved inorganic carbon pool dynamics in northern Gerlache Strait, Antarctica. Journal of Geophysical Research 104, 15873–15884.

Cefarelli, A., Vernet, M., Ferrario, M.E., Phytoplankton composition and abundance in relation to free-floating Antarctic icebergs. Deep-Sea Research II, this issue [doi:10.1016/j.dsr2.2010.11.023].

Chisholm, S.W., 1992. Phytoplankton size. In: Falkowski, P.G., Woodhead, D.D. (Eds.), Primary Productivity and Biogeochemical Cycles in the Sea. Plenum Press, New York, pp. 213–237.

Coale, K.H., Johnson, K.S., Chavez, F.P., Buesseler, K.O., Barber, R.T., Brzezinski, M.A., Cochlan, W.P., Millero, F.J., Falkowski, P.G., Bauer, J.E., Wanninkhof, R.H., Kudela, R.M., Altabet, M.A., Hales, B.E., Takahashi, T., Landry, M.R., Bidigare, R.R., Wang, X.J., Chase, Z., Strutton, P.G., Friederich, G.E., Gorbunov, M.Y., Lance, V.P., Hilting, A.K., Hiscock, M.R., Demarest, M., Hiscock, W.T., Sullivan, K.F., Tanner, S.J., Gordon, R.M., Hunter, C.N., Elrod, V.A., Fitzwater, S.E., Jones, J.L., Tozzi, S., Koblizek, M., Roberts, A.E., Herndon, J., Brewster, J., Ladizinsky, N., Smith, G., Cooper, D., Timothy, D., Brown, S.L., Selph, K.E., Sheridan, C.C., Twining, B.S., Johnson, Z.I., 2004. Southern ocean iron enrichment experiment: carbon cycling in high- and low-Si waters. Science 304, 408–414.

Daniels, R.M., Richardson, T.L., Ducklow, H.W., 2006. Food web structure and biogeochemical processes during oceanic phytoplankton blooms: an inverse model analysis. Deep-Sea Research II 53, 532–554.

de Baar, H.J.W., 1995. Importance of iron for phytoplankton blooms and carbon-dioxide drawdown in the Southern-Ocean. Nature 373, 412.

Dierssen, H.M., Vernet, M., Smith, R.C., 2000. Optimizing models for remotely estimating primary production in Antarctic coastal waters. Antarctic Science 12, 20–32.

DiTullio, G.R., Geesey, M.E., Maucher, J.M., Alm, M.B., Riseman, S.F., Bruland, K.W., 2005. Influence of iron on algal community composition and physiological status in the Peru upwelling system. Limnology and Oceanography 50 (6), 1887–1907.

Donaldson, P.B., 1978. Melting of Antarctic icebergs. Nature 275, 305–306.

Dubischar, C.D., Bathmann, U.V., 1997. Grazing impact of copepods and salps on phytoplankton in the Atlantic sector of the Southern Ocean. Deep-Sea Research II 44, 415–433.

Dunbar, M.J., 1984. The biological significance of Arctic ice. In: vanAlstine, E., Cook, A., (Eds.). Canadian Arctic Resources Committee Workshop, April 1982, Montreal, Quebec, pp. 7–30.

Ehnert, W., McRoy, C.P., 2007. Phytoplankton biomass and size fractions in surface waters of the Australian sector of the Southern Ocean. Journal of Oceanography 63, 179–187.

El Sayed, S.Z., Taguchi, S., 1981. Primary production and standing crop of phytoplankton along the ice-edge in the Weddell Sea. Deep-Sea Research-Oceanographic Research Papers 28A, 1017–1032.

Eppley, R.W., 1972. Temperature and phytoplankton growth in sea. Fishery Bulletin 70, 1063–1085.

Falkowski, P.G. (Ed.), 1980. Primary Productivity in the Sea: Environmental Science Research, vol. 19. Plenum Press, New York.

Fiala, M., Semeneh, M., Oriol, L., 1998. Size-fractionated phytoplankton biomass and species composition in the Indian sector of the Southern Ocean during the austral summer. Journal of Marine Systems 17, 179–194.

Figueiras, F.G., Estrada, M., Lopez, O., Arbones, B., 1998. Photosynthetic parameters and primary production in the Bransfield Strait: relationships with mesoscale hydrographic structures. Journal of Marine Systems 17, 129–141.

Froneman, P.W., Pakhomov, E.A., Balarin, M.G., 2004. Size-fractionated phytoplankton biomass, production and biogenic carbon flux in the eastern Atlantic sector of the Southern Ocean in late austral summer 1997–1998. Deep-Sea Research II 51, 2715–2729.

Fryxell, G.A., 1989. Marine-phytoplankton at the Weddell Sea ice edge—seasonal-changes at the specific level. Polar Biology 10, 1–18.

Fryxell, G.A., Kendrick, G.A., 1988. Austral spring microalgae across the Weddell Sea ice edge–spatial relationships found along a northward transect during Ameriez-83. Deep-Sea Research 35A, 1–20.

Gall, M.P., Boyd, P.W., Hall, J., Safi, K.A., Chang, H., 2001. Phytoplankton processes. Part 1: Community structure during the Southern Ocean Iron RElease Experiment (SOIREE). Deep-Sea Research II 48, 2551–2570.

Garibotti, I.A., Vernet, M., Ferrario, M.E., Smith, R.C., Ross, R.M., Quetin, L.B., 2003a. Phytoplankton spatial distribution in the Western Antarctic Peninsula (Southern Ocean). Marine Ecology Progress Series 261, 21–39.

Garibotti, I.A., Vernet, M., Kozlowski, W.A., Ferrario, M.E., 2003b. Composition and biomass of phytoplankton assemblages in coastal Antarctic waters: a comparison of chemotaxonomic and microscopic analyses. Marine Ecology Progress Series 247, 27–42.

Gladstone, R.M., Bigg, G.R., Nicholls, K.W., 2001. Iceberg trajectory modeling and meltwater injection in the Southern Ocean. Journal of Geophysical Research 106, 19903–19915.

Gordon, A.L., 1998. Western Weddell Sea thermohaline stratification. In: Jacobs, S.S., Weiss, R.F. (Eds.), Ocean, Ice and Atmosphere:Interactions at the Antarctic Continental Margin. American Geophysical Union, Washington, DC, pp. 215–240.

Hegseth, E.N., Von Quillfeldt, C.H., 2002. Low phytoplankton biomass and ice algal blooms in the Weddell Sea during the ice-filled summer of 1997. Antarctic Science 14, 231–243.

Helbling, E.W., Villafane, V., Holm-Hansen, O., 1991. Effect of iron on productivity and size distribution of Antarctic phytoplankton. Limnology and Oceanography 36, 1879–1885.

Helly, J., Kaufmann, R., Stephenson, G., Vernet, M., Cooling, dilution and mixing of ocean water by free-drifting icebergs in the Weddell Sea. Deep-Sea Research II, this issue [doi:10.1016/j.dsr2.2010.11.010].

Hernandez-Leon, S., Montero, I., Almeida, C., Portillo-Hahnefeld, A., Bruce-Lauli, E., 2008. Mesozooplankton biomass and indices of grazing and metabolic activity in Antarctic waters. Polar Biology 31, 1373–1382.

Hewes, C.D., 2009. Cell size of Antarctic phytoplankton as a biogeochemical condition. Antarctic Science 21 (5), 457–470.

Holm-Hansen, O., Lorenzen, C., Homes, R., Strickland, J., 1965. Fluorometric determination of chlorophyll. Journal du Conseil 30, 3–15.

Holm-Hansen, O., Amos, A.F., Silva, N., Villafañe, V.E., Helbling, E.W., 1994. In situ evidence for a nutrient limitation of phytoplankton growth in pelagic Antarctic waters. Antarctic Science 6, 315–324.

Hooper, R., 1971. Biological features in the iceberg environment. In: Proceedings of the Canadian Seminar on Icebergs, held at the Canadian Forces Maritime Warfare School, 6–7 December, Halifax, Nova Scotia, p. 112.

Hopkinson, B.M., Mitchell, B.G., Reynolds, R.A., Wang, H., Selph, K.E., Measures, C.I., Hewes, C.D., Holm-Hansen, O., Barbeau, K.A., 2007. Iron limitation across chlorophyll gradients in the southern Drake Passage: phytoplankton responses to iron addition and photosynthetic indicators of iron stress. Limnology and Oceanography 52, 2540–2554.

Jeffrey, S.W., Humphrey, G.F., 1975. New spectrophotometric equations for determining chlorophylls a, B, C1 and C2 in higher-plants, algae and natural phytoplankton. Biochemie und Physiologie Der Pflanzen 167, 191–194.

Jenkins, A., 1999. The impact of melting ice on ocean waters. Journal of Physical Oceanography 29, 2370–2381.

Kang, S.H., Fryxell, G.A., 1993. Phytoplankton in the Weddell Sea, Antarctica—composition, abundance and distribution in water-column assemblages of the marginal ice-edge zone during austral autumn. Marine Biology 116, 335–348.

Kang, S.H., Kang, J.S., Lee, S., Chung, K.H., Kim, D., Park, M.G., 2001. Antarctic phytoplankton assemblages in the marginal ice zone of the northwestern Weddell Sea. Journal of Plankton Research 23, 333–352.

Kang, S.H., Lee, S.H., 1995. Antarctic phytoplankton assemblage in the western Bransfield Strait region, February 1993: composition, biomass and mesoscale distributions. Marine Ecology Progress Series 129, 253–267.

Kaufmann, R.S., Robison, B.H., Sherlock, R.S., Reisenbichler, K.R., Osborn, K., Composition and structure of macrozooplankton and micronekton communities in the vicinity of free-drifting Antarctic icebergs. Deep-Sea Research II, this issue [doi:10.1016/j.dsr2.2010.11.026].

Kawaguchi, S., Shiomoto, A., Imai, K., Tsarina, Y., Yamaguchi, H., Noiri, Y., Iguchi, N., Kameda, T., 2000. A possible explanation for the dominance of chlorophyll in pico and nano-size fractions in the waters around the South Shetland Islands. Ocean and Polar Research 23 (4), 379–388.

Krell, A., Schnack-Schiel, S.B., Thomas, D.N., Kattner, G., Wang, Z.P., Dieckmann, G.S., 2005. Phytoplankton dynamics in relation to hydrography, nutrients and zooplankton at the onset of sea ice formation in the eastern Weddell Sea (Antarctica). Polar Biology 28, 700–713.

Knox, G.A., 2007. Biology of the Southern Ocean, 2nd edition CRC Press, Boca Raton, FL.

Lancelot, C., de Montety, A., Goosse, H., Becquevort, S., Schoemann, V., Pasquer, B., Vancoppenolle, M., 2009. Spatial distribution of the iron supply to phytoplankton in the Southern Ocean: a model study. Biogeosciences 6, 2861–2878.

Lin, H., Rauschenberg, S., Hexel, C.R., Shaw, T.J., Twining, B.S., Free-drifting icebergs as sources of iron to the Weddell Sea. Deep-Sea Research II, this issue [doi:10.1016/j.dsr2.2010.11.020].

Loeb, V., Siegel, V., Holm-Hansen, O., Hewitt, R., Fraser, W., Trivelpiece, W., Trivelpiece, S., 1997. Effects of sea-ice extent and krill or salp dominance on the Antarctic food web. Nature 387, 897–900.

Longhurst, A.R., 1998. Ecological Geography of the Sea. Academic Press, San Diego, CA.

Please cite this article as: Vernet, M., et al., Impacts on phytoplankton dynamics by free-drifting icebergs in the NW Weddell Sea. Deep-Sea Research II (2011), doi:10.1016/j.dsr2.2010.11.022

Lorenzen, C.J., 1967. Vertical distribution of chlorophyll and phaeopigments: Baja California. Deep Sea Research 14, 735–745.
Martin, J.H., Gordon, R.M., Fitzwater, S.E., 1990. Iron in antarctic waters. Nature 345, 156–158.
Mitchell, B.G., Holm-Hansen, O., 1991. Observations and modeling of the Antarctic phytoplankton crop in relation to mixing depth. Deep-Sea Research 38, 981–1007.
Montero, P., Daneri, G., Cuevas, L.A., Gonzalez, H.E., Jacob, B., Lizarraga, L., Menschel, E., 2007. Productivity cycles in the coastal upwelling area off Concepcion: The importance of diatoms and bacterioplankton in the organic carbon flux. Progress in Oceanography 75, 518–530.
Neshyba, S., 1977. Upwelling by icebergs. Nature 267, 507–508.
Pakhomov, E.A., Dubischar, C.D., Strass, V., Brichta, M., Bathmann, U.V., 2006. The tunicate *Salpa thompsoni* ecology in the Southern Ocean: Distribution, biomass, demography and feeding ecophysiology. Marine Biology 149, 609–623.
Park, M.G., Yang, S.R., Kang, S.H., Chung, K.H., Shim, J.H., 1999. Phytoplankton biomass and primary production in the marginal ice zone of the northwestern Weddell Sea during austral summer. Polar Biology 21, 251–261.
Parker, B.C., Heiskell, L.E., Thompson, W.J., 1978. Non-biogenic fixed nitrogen in Antarctica and some ecological implications. Nature 271, 651–652.
Patton, C.J., 1983. Design, characterization and applications of a miniature continuous flow analysis system. Ph.D. Thesis, Michigan State University, U. Microfilms International, Ann Arbor, Michigan, 150 pp.
Quetin, L.B., Ross, R.M., Fritsen, C.H., Vernet, M., 2007. Ecological responses of Antarctic krill to environmental variability: can we predict the future? Antarctic Science 19, 253–266.
Rhodes, R.H., Bertler, N.A.N., Baker, J.A., Sneed, S.B., Oerter, H., Arrigo, K.R., 2009. Sea ice variability and primary productivity in the Ross Sea, Antarctica, from methylsulphonate snow record. Geophysical Research Letters 36, L10704.
Robe, R.Q., 1978. Upwelling by icebergs. Nature 271 (16), 687.
Roberts, D., Craven, M., Cai, M.H., Allison, I., Nash, G., 2007. Protists in the marine ice of the Amery Ice Shelf, East Antarctica. Polar Biology 30, 143–153.
Rodriguez, J., Tintore, J., Allen, J.T., Blanco, J.M., Gomis, D., Reul, A., Ruiz, J., Rodriguez, V., Echevarria, F., Jimenez-Gomez, F., 2001. Mesoscale vertical motion and the size structure of phytoplankton in the ocean. Nature 410, 360–362.
Ross, R.M., Quetin, L.B., Baker, K.S., Vernet, M., Smith, R.C., 2000. Growth limitation in young *Euphausia superba* under field conditions. Limnology and Oceanography 45 (1), 31–43.
Schodlok, M.P., Hellmer, H.H., Rohardt, G., Fahrbach, E., 2006. Weddell Sea iceberg drift: five years of observations. Journal of Geophysical Research 111, C06018. doi:10.1029/2004JC002661.
Schwarz, J.N., Schodlok, M.P., 2009. Impact of drifting icebergs on surface phytoplankton biomass in the Southern Ocean: ocean colour remote sensing and *in situ* iceberg tracking. Deep-Sea Research I 56, 1727–1741.
Shaw, T.J., Hexel, C.R., Smith, K.L., Sherman, A.D., Dudgeon, R., Vernet, M., Kaufmann, R.S., $^{234}$Th-based carbon export around free-drifting icebergs in the Southern Ocean. Deep Sea Research II, this issue [doi:10.1016/j.dsr2.2010.11.019].
Shulenberger, E., 1983. Water-column studies near a melting arctic iceberg. Polar Biology 2 (3), 149–158.
Sedwick, P.N., DiTullio, G.R., 1997. Regulation of algal blooms in Antarctic shelf waters by the release of iron from melting sea ice. Geophysical Research Letters 24, 2515–2518.
Smith, K., Robison, B.H., Helly, J.J., Kaufmann, R.S., Ruhl, H.A., Shaw, T.J., Twining, B.S., Vernet, M., 2007. Free-drifting icebergs: Hot spots of chemical and biological enrichment in the Weddell Sea. Science 317, 478–482.
Smith, K.L., Sherman, A.D., Shaw, T., Murray, A., Vernet, M., Cefarelli, A., Carbon export associated with free-drifting icebergs in the Southern Ocean. Deep-Sea Research II, this issue [doi:10.1016/j.dsr2.2010.11.027].
Smith, W.O., Lancelot, C., 2004. Bottom-up versus top-down control in phytoplankton of the Southern Ocean. Antarctic Science 16 (4), 531–539.
Smith, W.O., Nelson, D.M., 1985. Phytoplankton bloom produced by receding ice edge in the Ross Sea: spatial coherence with the density field. Science 227, 163–165.
Smith, W.O., Nelson, D.M., 1990. Phytoplankton growth and new production in the Weddell Sea Marginal Ice-Zone in the austral spring and autumn. Limnology and Oceanography 35, 809–821.
Stephenson, G.R., Sprintall, J., Gille, S.T., Vernet, M., Helly, J.J., Kaufmann, R.S., Subsurface melting of a free-floating Antarctic iceberg. Deep-Sea Research II, this issue [doi:10.1016/j.dsr2.2010.11.009].
Stuart, K.M., Long, D.G., Tracking large tabular icebergs using the SeaWinds Ku-band microwave scatterometer. Deep Sea Research II, this issue [doi: 10.1016/j.dsr2.2010.11.004].
Tagliabue, A., Arrigo, K.R., 2006. Processes governing the supply of iron to phytoplankton in stratified seas. Journal of Geophysical Research 111, C06019.
Tremblay, J.-E., Legendre, L., 1994. A model for the size-fractionated biomass and production of marine phytoplankton. Limnology and Oceanography 39 (8), 2004–2014.
Varela, M., Fernandez, E., Serret, P., 2002. Size-fractionated phytoplankton biomass and primary production in the Gerlache and south Bransfield Straits (Antarctic Peninsula) in Austral summer 1995–1996. Deep-Sea Research II 49, 749–768.
Vernet, M., Martinson, D., Iannuzzi, R., Stammerjohn, S., Kozlowski, W., Sines, K., Smith, R., Garibotti, I., 2008. Primary production within the sea-ice zone west of the Antarctic Peninsula: I-Sea ice, summer mixed layer, and irradiance. Deep-Sea Research II 55, 2068–2085.
Walsh, J.J., Dieterle, D.A., Lenes, J., 2001. A numerical analysis of carbon dynamics of the Southern Ocean phytoplankton community: the roles of light and grazing in effecting both sequestration of atmospheric $CO_2$ and food availability to larval krill. Deep-Sea Research I 48, 1–48.
Welschmeyer, N.A., Lorenzen, C.J., 1985. Chlorophyll budgets: zooplankton grazing and phytoplankton growth in a temperate fjord and the Central Pacific Gyres. Limnology and Oceanography 30, 1–21.
Whitaker, T.M., 1977. Sea ice habitats of Signy Island (South Orkneys) and their primary productivity. In: Llano, G.A. (Ed.), Adaptations within Antarctic Ecosystems. Gulf Publ. Co., pp. 75–82.

Please cite this article as: Vernet, M., et al., Impacts on phytoplankton dynamics by free-drifting icebergs in the NW Weddell Sea. Deep-Sea Research II (2011), doi:10.1016/j.dsr2.2010.11.022